

Review

Diphenyl Carbonate: Recent Progress on Its Catalytic Synthesis by Transesterification

Dong Wang^{1,2}, Feng Shi^{1,3,*} and Guochao Yang^{3,*}¹ Tianjin Jiuyuan Chemical Engineering Co., Ltd., Tianjin 300384, China² Technical Quality Department, Rongsheng New Materials (Zhoushan) Co., Ltd., Zhoushan 316000, China³ Key Laboratory for Green Chemical Technology of MOE, Tianjin University, Tianjin 300072, China

* Correspondence: alexei@tju.edu.cn (F.S.); yang_gc@tju.edu.cn (G.Y.); Tel.: +86-22-27406119 (G.Y.)

Abstract: Diphenyl carbonate is one of the raw materials used for the synthesis of polycarbonate, and its green and clean production is of great importance to the non-phosgene process for polycarbonate. The production of diphenyl carbonate by transesterification is its representative process route and is considered to be one of the typical examples of a green and sustainable process for chemicals. Since the discovery of the transesterification catalyst for diphenyl carbonate in the 1970s, researchers have been committed to improving its catalytic activity and selectivity and, correspondingly, the reaction engineering process. However, thermodynamic limitations, low activity, low selectivity, and limited stability have been bottlenecks that the transesterification catalyst has not been able to completely overcome, and the improvement of the catalyst is still ongoing. Therefore, this review takes the transesterification reaction of dimethyl carbonate and phenol as a model reaction and, based on a review of the progress in catalyst research on catalytic reaction processes, tries to clarify the structure–activity relationship between catalytic active sites and catalytic performance in homogeneous and heterogeneous catalytic processes and provides an overview of the progress in catalyst synthesis and modification.

Keywords: diphenyl carbonate; transesterification; Lewis acid catalysis; polycarbonate



Citation: Wang, D.; Shi, F.; Yang, G. Diphenyl Carbonate: Recent Progress on Its Catalytic Synthesis by Transesterification. *Catalysts* **2024**, *14*, 250. <https://doi.org/10.3390/catal14040250>

Academic Editor: Guido Busca

Received: 15 March 2024

Revised: 3 April 2024

Accepted: 4 April 2024

Published: 9 April 2024



Copyright: © 2024 by the authors. Licensee MDPI, Basel, Switzerland. This article is an open access article distributed under the terms and conditions of the Creative Commons Attribution (CC BY) license (<https://creativecommons.org/licenses/by/4.0/>).

1. Introduction to Diphenyl Carbonate

Polycarbonate is a common engineering plastic. Due to its good optical and mechanical properties [1,2], it is widely used in civilian fields [3–5] for products such as discs, automotive components, sports equipment shells, outdoor curtain walls, and water bottles [6–9]. With the development of new energy technology, polycarbonate materials have become particularly important for new energy vehicles, leading to a continuous increase in annual production. By the 2020s, the annual production of polycarbonate had reached 7.5 million tons, and new capacity plans have been continuously proposed.

Currently, there are two production methods for polycarbonate, namely, the phosgene method and the transesterification method [10–12]. In the phosgene method, bisphenol A reacts with phosgene at the interface of a NaOH solution solvent to form polycarbonate. The main problem is the large amount of solvent, represented by dichloromethane, which increases material and energy consumption. Additionally, the use of highly toxic phosgene leads to environmental and safety issues. On the other hand, the transesterification method involves the reaction of bisphenol A and diphenyl carbonate (DPC) in a molten state, resulting in a simple process, no need for solvents, environmental friendliness, and uniform molecular weight and meeting requirements for higher product grades. Therefore, it is the future development direction of polycarbonate technology.

The source of diphenyl carbonate is crucial in the transesterification process. Currently, the main production processes for diphenyl carbonate include the phosgene method and the transesterification method [13–15]. The phosgene method involves the generation of

chloroformic acid benzyl ester from benzene and phosgene in a NaOH solution, which is further condensed with benzene to produce diphenyl carbonate. This process is relatively mature, but the use of highly toxic phosgene limits its further development. In the transesterification process, phenol (PhOH) and dimethyl carbonate (DMC) undergo transesterification to produce diphenyl carbonate and methanol. Dimethyl carbonate is obtained from the oxidation–carbonylation of methanol, and the raw materials used in this process are non-toxic, non-polluting, and non-corrosive, making it an ideal process route for the production of diphenyl carbonate.

Currently, the transesterification process is replacing the phosgene method and becoming a representative of environmentally friendly and pollution-free green chemical processes. In the transesterification process, the catalyst is crucial and directly affects the product selectivity and subsequent separation efficiency. This review focuses on catalysts used for the preparation of diphenyl carbonate via the transesterification method.

2. Reaction Pathways and Reaction Thermodynamics of Transesterification of Phenol with Dimethyl Carbonate

2.1. Reaction Pathways for Transesterification

The general transesterification reaction equation of phenol and DMC is [14,16–18] shown by (1) in Figure 1:

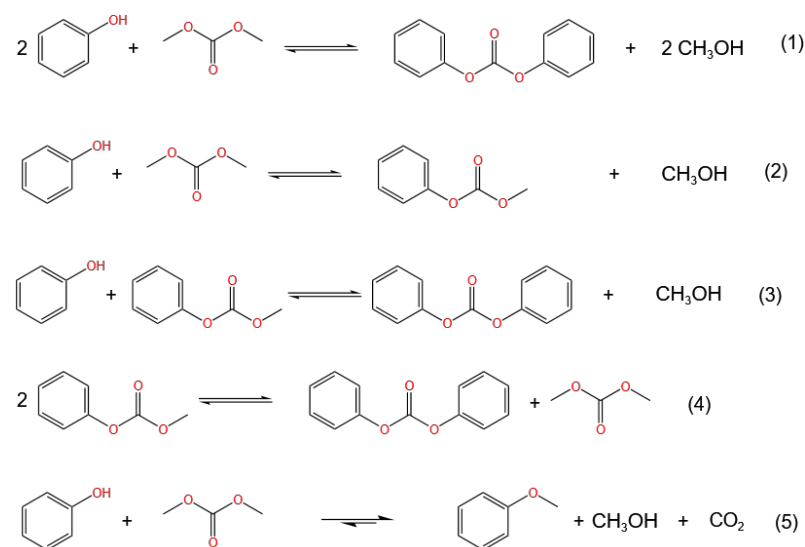


Figure 1. General reaction equation and scheme for transesterification of phenol and DMC.

This reaction includes the following steps:

DMC reacts with phenol to form methyl phenyl carbonate (MPC) through transesterification, shown by (2) in Figure 1. MPC and phenol are subjected to the transesterification reaction again to generate DPC, shown by (3) in Figure 1, or MPC undergoes a self-disproportionation reaction to generate DMC and DPC, shown by (4) in Figure 1.

The main side reaction is the formation of anisole from DMC and phenol, shown by (5) in Figure 1.

2.2. Thermodynamic Analysis of Transesterification

2.2.1. Methodology of Thermodynamic Analysis

To elucidate the maximum extent to which transesterification can proceed, researchers first conduct a thermodynamic analysis of the reaction. Currently, the most common approach involves using theoretical methods to compute the relevant parameters, such as standard enthalpy and entropy changes, which, in turn, yield the Gibbs free energy change for transesterification. Ultimately, this leads to the equilibrium constant (K), determined through Equation (1):

$$\Delta G = -RT \ln K, \quad (1)$$

For instance, Zhang et al. [19] combined molecular simulation with process simulation software, employing both Benson's group contribution method and Joback and Reid's group contribution method to calculate the liquid formation heat of individual substances, thereby obtaining the reaction enthalpy change. They used the Dmol3 module within Material Studio to acquire the standard formation enthalpies of the substances, thus deducing the reaction entropy change based on statistical thermodynamics. Li et al. [20], on the other hand, relied on previously reported data from the literature and utilized extensive properties to design computational pathways to derive the reaction enthalpy and entropy changes. In contrast, Yang et al. [21] directly employed Density Functional Theory (DFT) calculations using Gaussian 09 software to obtain all the formation enthalpies and formation entropies of the related substances in the reaction, thus determining the reaction enthalpy and entropy changes.

Apart from theoretical methods, some researchers have also adopted experimental approaches to directly measure the reaction enthalpy change and subsequently determine the equilibrium constant. For example, Haubrock et al. [22] and Zhao et al. [23] separately used batch reactors in their experiments to directly measure the reaction equilibrium constants.

2.2.2. Thermodynamic Constraint in Transesterification by Calculation

Multiple calculations have shown that transesterification between dimethyl carbonate and phenol is thermodynamically limited, with a small equilibrium constant. Li et al. [20] used the group contribution method to calculate the standard Gibbs free energies and entropies of phenol, dimethyl carbonate, and diphenyl carbonate and then calculated the reaction enthalpy, entropy change, Gibbs free energy change, and equilibrium constant of the transesterification reaction, as shown in Table 1.

Table 1. Reaction enthalpies, entropy changes, Gibbs free energy changes, and equilibrium constants for transesterification at different temperatures (data from [20]).

| Temperature/°C | $\Delta_r G_m^0/\text{kJ}\cdot\text{mol}^{-1}$ | $\Delta_r H_m^0/\text{kJ}\cdot\text{mol}^{-1}$ | $\Delta_r S_m^0/\text{J}\cdot\text{mol}^{-1}\cdot\text{K}^{-1}$ | K |
|----------------|--|--|---|-----------------------|
| 25 | 65.4 | 64.4 | −3.6 | 3.5×10^{-12} |
| 100 | 25.2 | 49.6 | 65.3 | 2.9×10^{-4} |
| 150 | 22.2 | 45.9 | 56 | 1.8×10^{-3} |
| 180 | 20.8 | 43 | 49.1 | 4.0×10^{-3} |
| 220 | 26.8 | 45.2 | −146.1 | 1.4×10^{-3} |
| 250 | 28.8 | 41.2 | −133.9 | 1.3×10^{-3} |

The table provided illustrates that the transesterification reaction displays endothermic characteristics when the temperature remains below 180 °C. As the temperature increases, the reaction becomes more favorable. Conversely, when the temperature exceeds 180 °C, the reaction becomes exothermic, resulting in decreased favorability. Therefore, the reaction proceeds optimally at approximately 180 °C. At this temperature, the reaction equilibrium constant reaches its maximum value, albeit at a modest figure of 4×10^{-3} . Consequently, this reaction is considered to be thermodynamically challenging to promote.

Simultaneously, thermodynamic calculations for the side reaction leading to the production of anisole (as demonstrated in Table 2) show that spontaneous occurrence is possible within the temperature range of 25–250 °C. Furthermore, at 180 °C, the equilibrium constant attains a significantly higher value of 7.60×10^6 compared to the main reaction equilibrium constant, indicating greater thermodynamic favorability. Therefore, achieving a high selectivity for diphenyl carbonate primarily depends on suppressing the formation of anisole.

Table 2. Reaction enthalpies, entropy changes, Gibbs free energy changes, and equilibrium constants for reactions to produce anisole at different temperatures (data from [20]).

| Temperature/°C | $\Delta_r G_m^0/\text{kJ}\cdot\text{mol}^{-1}$ | $\Delta_r H_m^0/\text{kJ}\cdot\text{mol}^{-1}$ | $\Delta_r S_m^0/\text{J}\cdot\text{mol}^{-1}\cdot\text{K}^{-1}$ | K |
|----------------|--|--|---|---------------------|
| 25 | −32.6 | 25.9 | 192.9 | 5.1×10^5 |
| 100 | −45.7 | 10.7 | 151.1 | 2.50×10^6 |
| 150 | −53.5 | 13.4 | 158.2 | 4.10×10^6 |
| 180 | −59.7 | 52.5 | 247.6 | 7.60×10^6 |
| 220 | −65.7 | 10.7 | 154.9 | 9.10×10^6 |
| 250 | −71.8 | 14.8 | 165.6 | 15.00×10^6 |

Yang et al. [21] calculated the liquid formation enthalpies and standard entropies of all substances in the reaction using DFT and calculated the standard Gibbs free energy change for the reaction. The results showed that within the temperature range of 25–200 °C, the pathway of MPC disproportionation to form DPC was relatively favorable, while the pathway of MPC continuing transesterification to DPC was relatively difficult.

Zhang et al. [19] and Zhao et al. [23] also calculated the equilibrium constant for the transesterification reaction at 180 °C and obtained values of 1.25×10^{-4} and 1.23×10^{-3} , respectively. Although there is a difference in the calculated results (which may be due to the different calculation methods), the equilibrium constant for the transesterification is still very small. This also indicates that the transesterification is indeed a thermodynamically unfavorable reaction, and some measures need to be taken in the catalytic process, such as using reactive distillation during the reaction to continuously remove the formed methanol product, to promote the movement of the equilibrium [15,24].

3. Homogeneous Catalysts for Transesterification

The research and industrialization of catalysts for transesterification originated in the 1970s. The first effective catalysts discovered were homogeneous catalysts such as metal halides or alcohol salts. Enichem first disclosed the use of halides, alcohol salts, and acetylacetonate derivatives containing metals such as Al, Ti, Sn, and V to catalyze the disproportionation reaction of methyl phenyl carbonate. Titanium tetrabutoxide was used as a catalyst, achieving 93% selectivity at 180 °C. Subsequently, General Electric, Mitsubishi Chemical, Mitsui Chemicals, Bayer, and others also disclosed methods using titanium- or tin-based organometallics as catalysts. In addition, Asahi Kasei also disclosed a method using lead as the catalytically active component. The main catalytic active center for transesterification is the Lewis acid site [25–28]. According to the general mechanism of transesterification, the active site is a metal site with Lewis acidity. Therefore, the nature of the metal site determines the catalytic performance. Currently, based on the components of the catalysts, they can be classified into Ti-based, Sn-based, Pb-based, and rare-earth-metal-based catalysts.

3.1. Ti-Based Catalysts

Ti-based catalysts were the first proposed catalysts for transesterification, and the activity of Ti-based catalysts reported in the literature is summarized in Table 3.

The most commonly used titanium-based catalysts are titanium alkoxides. The catalytic activity of titanium alkoxides can be adjusted by the flexibility of their alkyl chains. Wang et al. [29] compared the activity between titanium tetrabutoxide and titanium tetraphenolate and found that titanium tetrabutoxide had better activity. This is because of the stronger electron-donating ability of butyl, making titanium tetrabutoxide more electron-donating, which is more conducive to the coordination between carbonyl and Ti(IV) and the transfer of electrons to metal ions. The authors proposed the reaction mechanism of titanium alkoxides, as shown in Figure 2. When the carbonyl group on dimethyl carbonate binds to Ti(IV) in the catalyst, electrons are transferred to Ti(IV), and the carbonyl group is polarized, making its carbon atom more susceptible to the nucleophilic attack of phenol. After coordinating with phenol, a four-membered ring transition state is

formed, and then the C-O bond breaks to form an O-H bond, producing MPC and methanol. Finally, the carbonyl group dissociates from Ti(IV), completing a catalytic reaction cycle. It can be seen that the strength of the coordination between the carbonyl group and Ti(IV) determines the reaction activity.

Table 3. Activity of homogeneous Ti-based catalysts.

| Catalyst | Temperature (°C) | Time (h) | PhOH/DMC | Cat/PhOH (in Mole) | Conversion ** (%) | MPC Yield (%) | DPC Yield (%) | Transesterification Selectivity *(%) | Ref. |
|---|------------------|----------|-----------|--------------------|-------------------|---------------|---------------|--------------------------------------|------|
| Ti(OBu) ₄ | 175 | 8 | 1 | 0.1 | 28.7 | 26.1 | 2.6 | 99.99 | [29] |
| Ti(OPh) ₄ | 175 | 8 | 1 | 0.1 | 25 | 23.1 | 1.9 | 100 | [29] |
| TiCp ₂ Cl ₂ | 150–180 | 10 | 1 | 0.005 | 46.8 | 20.3 | 25.7 | 98.3 | [30] |
| Ti(OEt) ₄ | 150–180 | 10 | 1 | 0.005 | 36.8 | 13.2 | 22.9 | 98.1 | [30] |
| Ti(OiPr) ₄ | 150–180 | 10 | 1 | 0.005 | 30 | 17.2 | 12.4 | 97.7 | [31] |
| CpTiCl ₃ | 150–180 | 10 | 1 | 0.005 | 40.2 | 20.3 | 25.7 | 98.3 | [31] |
| [(Me) ₅ Cp] ₂ TiCl ₂ | 150–180 | 10 | 1 | 0.005 | 30.7 | 16.2 | 22.6 | 96.5 | [31] |
| [(Me) ₅ Cp]TiCl ₃ | 150–180 | 10 | 1 | 0.005 | 6.8 | 17.4 | 12.9 | 100 | [31] |
| [(Et-Cp) ₂] ₂ TiCl ₂ | 150–180 | 10 | 1 | 0.005 | 40.2 | 6.8 | N.D. *** | 100 | [31] |
| [(Me) ₅ Cp]Ti(OMe) ₃ | 150–180 | 10 | 1 | 0.005 | 6.6 | 22.2 | 16.6 | 96.5 | [31] |
| Cp ₂ Ti(SO ₃ CF ₃) ₂ | 150–180 | 10 | 1 | 0.005 | 36.8 | 6.1 | 0.5 | 100 | [31] |
| [i-PrO] ₄ TiCl | 150–180 | 10 | 1 | 0.005 | 40.1 | 6.1 | 4.7 | 29.3 | [31] |
| Cp ₂ TiPh ₂ | 150–180 | 10 | 1 | 0.005 | 47.6 | 17.2 | 12.4 | 97.7 | [31] |
| Cp ₂ Ti(OPh) ₂ | 150–180 | 10 | 1 | 0.005 | 46 | 23.9 | 23.2 | 98.9 | [31] |
| TIBE | 185 | 3 | 0.125 | 0.0047 | 48.6 | 48.4 | N.D. *** | 99.5 | [17] |
| TBBE | 185 | 3 | 0.125 | 0.0047 | 50.7 | 50.4 | N.D. *** | 99.4 | [17] |
| TiO(OOCMe) ₂ | 150–180 | 9 | 1 | 0.0033 | 47.8 | 25.6 | 22.2 | 99.9 | [32] |
| TiCp ₂ Cl ₂ **** | 180 | 3 | N.A. **** | 0.04 | 31.4 | N.A. **** | 30.3 | 96.5 | [33] |
| TiO(acac) ₂ **** | 180 | 3 | N.A. **** | 0.04 | 69.2 | N.A. **** | 68.3 | 98.7 | [33] |
| TiO(OOCMe) ₂ **** | 180 | 3 | N.A. **** | 0.04 | 71.1 | N.A. **** | 69.5 | 97.7 | [33] |
| Ti(OBu) ₄ **** | 180 | 3 | N.A. **** | 0.04 | 86.2 | N.A. **** | 85.6 | 99.3 | [33] |
| Ti(OPh) ₄ **** | 180 | 3 | N.A. **** | 0.04 | 89.1 | N.A. **** | 87.8 | 98.5 | [33] |
| Ti(OiPr) ₄ **** | 180 | 3 | N.A. **** | 0.04 | 90.4 | N.A. **** | 90 | 99.6 | [33] |

* Transesterification selectivity includes both DPC and MPC. ** Conversion is calculated based on phenol unless stated otherwise. *** N.D. Not Detected. **** N.A. Not Available. ***** MPC disproportionation.

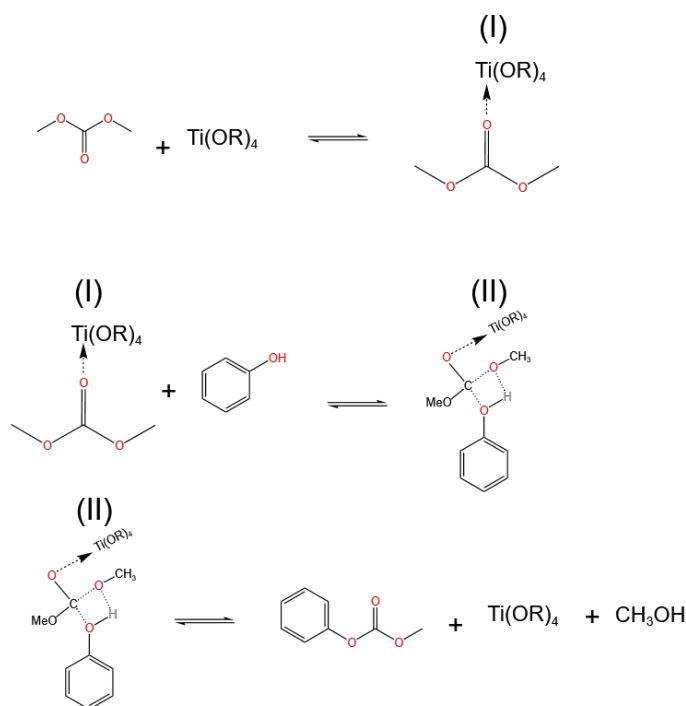


Figure 2. Mechanism of catalyzed transesterification reactions on titanates (redrawn, data from [29]).

Chen et al. [33] also compared the activity of MPC disproportionation to DPC with different alkoxy chain lengths of titanium alkoxides and proposed a structure–activity relationship between the coordination state of alkoxy titanium and catalytic activity. Both the steric hindrance and electronic effects of the coordinating groups collectively affect their catalytic performance. The electronic effect has a greater influence than steric hindrance. The smaller the steric hindrance of the coordinating group, the stronger the electron-withdrawing effect of the coordinating group, the stronger the Lewis acidity of titanium, and the higher the reactivity of titanium alkoxides, which is consistent with the above conclusion by Wang et al. [29]. However, excessively strong Lewis acids can easily lead to the decarboxylation of MPC to form anisole. Titanium tetraisopropoxide has the appropriate steric hindrance and electronic effects of coordinating groups, exhibiting the best catalytic performance. Based on this understanding, the authors also proposed a possible reaction mechanism of Lewis acid titanium compounds in the disproportionation reaction, as shown in Figure 3. Titanium first activates the oxygen of the carbonyl group to form a chelate, making the carbonyl carbon positively charged. Subsequently, it attacks another molecule of MPC, forming a four-atom transition-state Ti complex, which then undergoes nucleophilic substitution to generate DPC and DMC, completing the catalytic cycle.

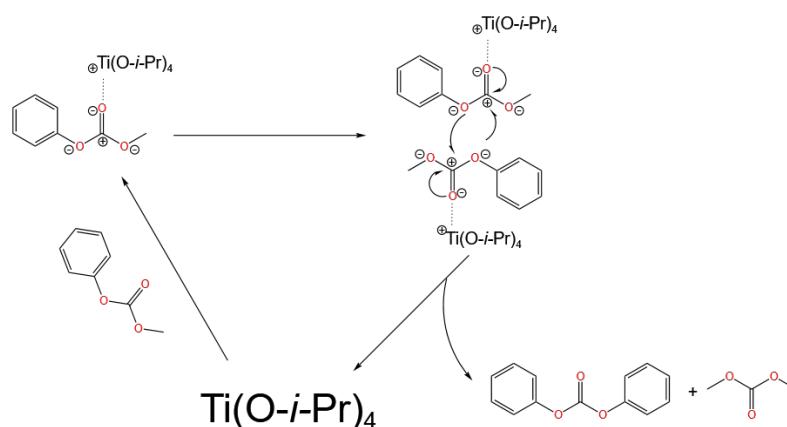


Figure 3. Mechanism of catalyzed MPC disproportionation reaction on titanates (redrawn, data from [33]).

Titanium alkoxides are highly susceptible to hydrolysis, leading to the formation of insoluble TiO_2 and the loss of catalytic activity. To overcome this drawback, Fang et al. [17] proposed the complexation of titanium alkoxides with acetylacetonate to substitute the alkoxy groups of titanium alkoxides with acac, aiming to enhance their water resistance. The structure of the prepared complex is shown in Figure 4. By enhancing transesterification through reaction distillation, they achieved an 86.4% conversion of phenol and a 99.4% selectivity of MPC, with significantly improved catalytic stability, showing no decline in activity after ten cycles of reuse. They also speculated that, with the complexed titanium catalyst, the reaction mechanism is similar to that with uncomplexed titanium ester catalysts, where the carbonyl group of dimethyl carbonate first coordinates with Ti(IV) and becomes polarized, indicating that complexed acetylacetonate did not change the reaction mechanism.

Other contributions also involve non-titanium ester catalysts. Wang et al. [30] proposed the use of air-stable dichlorodi(cyclopentadienyl)titanium (TiCp_2Cl_2) instead of titanium alkoxides as catalysts for transesterification. The reaction temperature was 150–180 °C, $\text{PhOH/DMC} = 1$, and the reaction time was 10 h. The conversion of phenol was 46.8%, and the selectivities of DPC and MPC were 54.9% and 43.4%, respectively. TiCp_2Cl_2 is widely used as an additive for olefin polymerization Ziegler–Natta catalysts, and it is easily commercially available and does not require any additional treatment before use. Under the reaction conditions, TiCp_2Cl_2 dissolves in the reaction system, but it can precipitate when cooled to room temperature, thus having significant advantages in catalyst separation. When comparing the activity of TiCp_2Cl_2 with that of titanium alkoxides, it

was found that its activity was also high. Two reasons were speculated: First, because the electron-withdrawing ability of the chlorine atom is stronger than that of the hydrocarbon group, Ti(IV) in TiCp_2Cl_2 has higher electrophilicity, namely, Lewis acidity, making the coordination of the carbonyl group of dimethyl carbonate with Ti(IV) easier. Second, the chlorine atom is smaller in size, thereby reducing the steric hindrance of Ti(IV), so Ti(IV) more readily participates in the reaction.

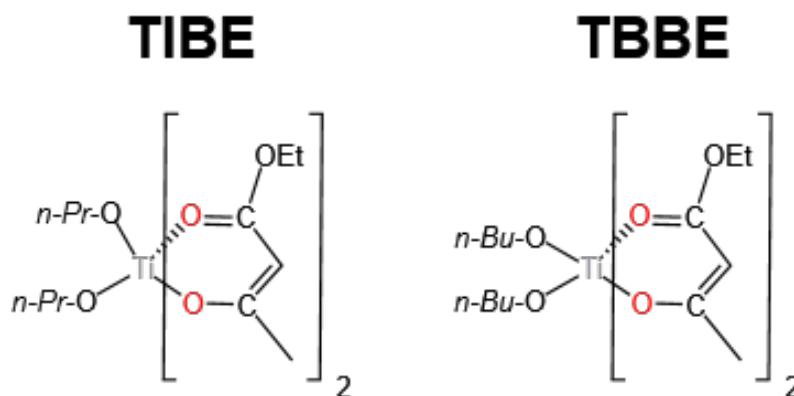


Figure 4. The structure of the product after the partial substitution of titanate by acetylacetonate (redrawn, data from [17]).

Subsequently, they also examined the catalytic activity of a series of cyclopentadienyltitanium compounds [31], studying the effects of substituents on the cyclopentadienyl ring and substituted chlorine atoms on the activity of cyclopentadienyltitanium compounds. The results showed that dichlorodi(cyclopentadienyl)titanium could achieve the highest yield of diphenyl carbonate. By summarizing the rules of the effects of activity, it was found that steric hindrance, the electronic dispersion effects of the cyclopentadienyl ring, and the electron-withdrawing effects of substituents connected to Ti(IV) all affect the Lewis acidity of Ti(IV) and the corresponding catalytic activity. Generally, the smaller the steric hindrance, the greater the electronic dispersion effect of the cyclopentadienyl ring, and the stronger the electron-withdrawing ability of the substituent connected to Ti(IV), the more favorable the reaction.

Additionally, Wang et al. [32] also discovered the catalytic activity of titanium acetylacetonate for transesterification, achieving a phenol conversion of 47.8% and a selectivity of over 99.9% for transesterification, with only trace amounts of the byproduct anisole detected. The characterization of the catalyst after the reaction revealed phenoxy titanium compounds. Therefore, they speculated that titanium acetylacetonate first reacted with phenol in the transesterification, and the phenoxy group substituted the acetate group to form phenoxy titanium compounds (as shown in Figure 5). Phenoxy titanium compounds are the actual catalysts for this transesterification, and a six-membered ring reaction mechanism was proposed (as shown in Figure 6).

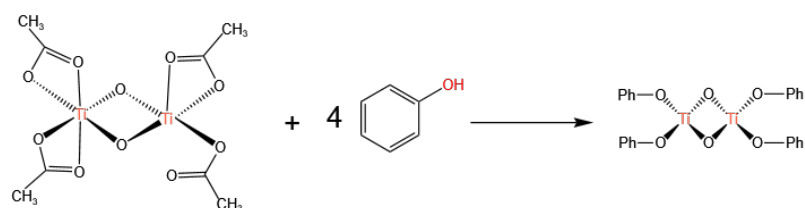


Figure 5. Structure of phenoxytitanium compounds produced by titanium oxyacetate and phenol (redrawn, data from [32]).

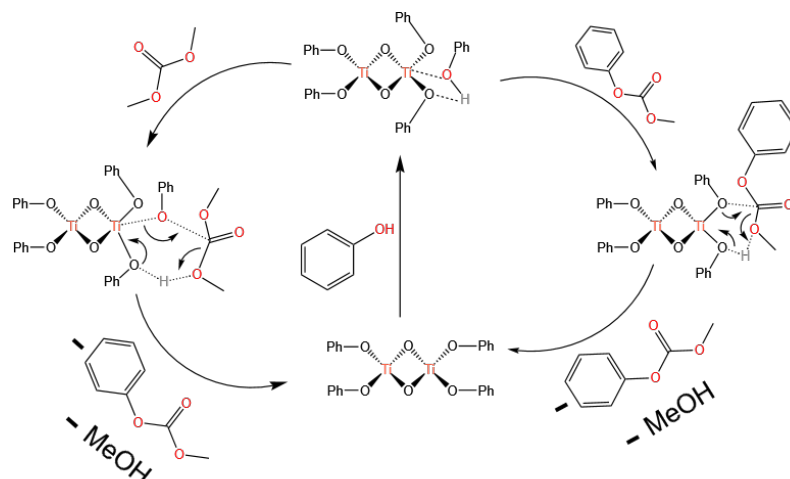


Figure 6. Mechanism of transesterification on phenoxytitanium compounds (redrawn, data from [32]).

3.2. Sn-Based Catalysts

Since the proposal of homogeneous transesterification catalysts in 1976, Sn-based catalysts, like Ti-based ones, have become ideal candidates for catalysis. The activity of Sn-based catalysts reported in the literature is summarized in Table 4.

Table 4. Activity of homogeneous Sn-based catalysts.

| Catalyst | Temperature (°C) | Time (h) | PhOH/DMC | Cat/PhOH (in Mole) | Conversion ** (%) | MPC Yield (%) | DPC Yield (%) | Transesterification Selectivity * (%) | Ref. |
|---|------------------|----------|----------|--------------------|-------------------|---------------|---------------|---------------------------------------|------|
| Bu ₂ SnO | 175 | 8 | 1 | 0.01 | 20.2 | 19.8 | 0.4 | 100 | [20] |
| Bu ₄ Sn | 175 | 8 | 1 | 0.01 | 0.1 | 0.1 | 0 | 100 | [20] |
| Bu ₂ SnO–CF ₃ SO ₃ H | 180 | 3 | 5 | 0.002 | 58.5 | 39.8 | 18.3 | 99.3 | [34] |
| Bu ₂ SnO–CH ₃ SO ₃ H | 180 | 3 | 5 | 0.002 | 56.5 | 36.5 | 19.7 | 99.5 | [34] |
| Bu ₂ SnO–CH ₃ C ₆ H ₄ SO ₃ H | 180 | 3 | 5 | 0.002 | 60.4 | 39.4 | 20.8 | 99.7 | [34] |
| Bu ₂ SnO–C ₆ H ₅ SO ₃ H | 180 | 3 | 5 | 0.002 | 57.9 | 38.2 | 19.4 | 99.5 | [34] |
| Bu ₂ SnO–Cu ₂ O | 150–180 | 8 | 2 | 0.008 | 50.8 *** | 35.4 | 15.4 | 99.9 | [35] |
| BuSn(O)OH–CuI | 150–180 | 8 | 2 | 0.0113 | 57.8 *** | 39.2 | 18.6 | 99.9 | [36] |

* Transesterification selectivity includes both DPC and MPC. ** Conversion is calculated based on phenol unless stated otherwise. *** Conversion is calculated based on DMC.

Sivaram et al. [37] compared the transesterification activities of various metals, including Ti, Sn, and Al, and the results showed that Sn has the best reaction activity, although with slightly lower selectivity. Li et al. [20], after comparing the catalytic activity of four different metals, supported the results of Sivaram et al. and preferred the catalyst to be dibutyltin oxide, with a DPC yield and selectivity of 43% and 88%, respectively. Wang et al. [38], after optimizing a series of Ti-, Sn-, and Pb-based catalysts, similarly selected dibutyltin oxide as having the highest catalytic activity. Subsequently, Wang et al. [39], using single-crystal XRD diffraction, proved the coordination structure formed by dibutyltin oxide in the reaction system, confirming it as a dimeric tetraalkyl distannoxane compound, shown in Figure 7, an intermediate in the transesterification. It was pointed out that the transesterification process consists of three steps: the generation of intermediates, transesterification (including the disproportionation of methyl phenyl carbonate), and the regeneration of intermediates. The research by Sivaram et al. [37] also supported the conclusion of Wang et al. [39] that dibutyltin oxide does not directly participate in the reaction; it first reacts with phenol to generate intermediates and then complexes with dimethyl carbonate to participate in the reaction.

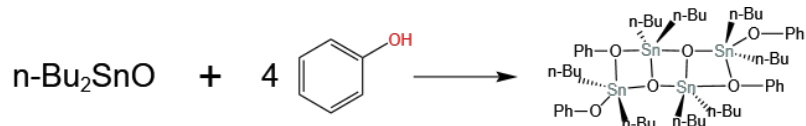


Figure 7. Reaction intermediates of dibutyltin oxide with phenol (redrawn, data from [39]).

Subsequently, researchers conducted various modifications on dibutyltin oxide. Kim et al. [34] found that adding alkyl or aryl sulfonic acids as additives to dibutyltin oxide can significantly increase its activity and reduce the selectivity of anisole. On the basis of ^{19}F MAS NMR and ^{119}Sn MAS NMR [40], they believed that, in the presence of phenol, dibutyltin oxide interacts with triflic acid to form active tin complexes containing triflic acid ligands. Therefore, the enhancement of the activity of dibutyltin oxide in the presence of alkyl or aryl sulfonic acids can be attributed to the formation of sulfonic acid-bonded tin, and its structure as $[\text{Bu}_2\text{Sn}(\text{OH})(\text{OTf})_2]$ and $[\text{Bu}_2\text{Sn}(\text{OAc})(\text{OTf})_2]$ was confirmed by single-crystal X-ray diffraction. The catalytic reaction mechanism was provided and is shown in Figure 8. The enhancement by aryl sulfonic acid is attributed to its electron-withdrawing property, which enhances the Lewis acidity of Sn(IV).

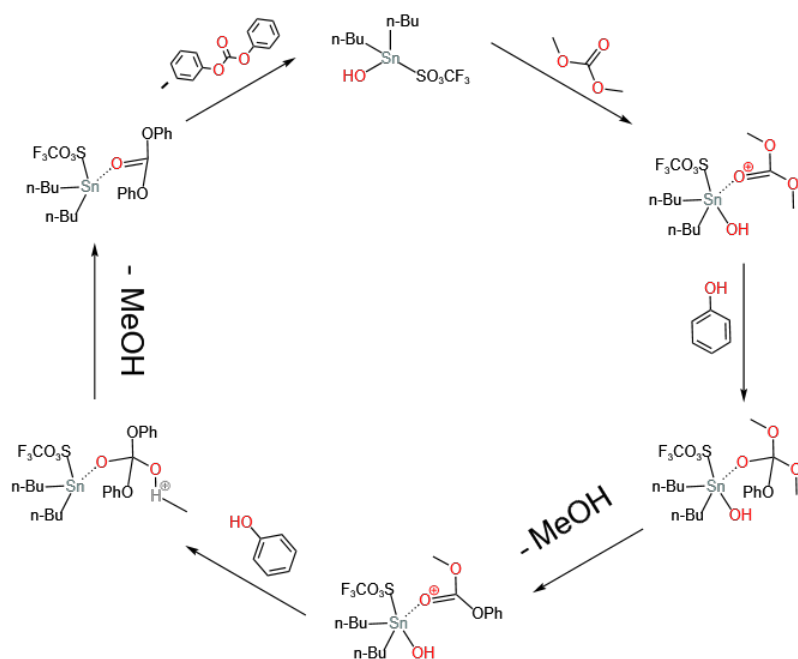


Figure 8. Reaction mechanism on homogeneous sulfonic acid-bonded tin catalyst (redrawn, data from [34]).

In addition, Wang et al. [36] also utilized Cu(I) salts in combination with dibutyltin hydroxide to enhance the activity and selectivity of transesterification. They compared different Cu(I) precursors ($\text{Cu}_2\text{O} < \text{CuCl} < \text{CuBr} < \text{CuI}$) and pointed out that the stronger the electronegativity of the anion in the additive, the weaker the promoting effect of the corresponding cuprous compound. Furthermore, they used this strategy to modify dibutyltin oxide [35] and found that Cu_2O could significantly enhance its activity, with a conversion of dimethyl carbonate as high as 50.8% and a selectivity of transesterification reaching 99.9%. They attempted to explain these phenomena using the hard and soft acid–base theory, finding that the transesterification is a combination of soft bases and hard acids. Dibutyltin oxide can be considered a hard acid, while Cu(I) can be considered a soft base to promote the catalytic activity of the hard acid.

3.3. Lead-Based Catalysts

In the 1990s, Asahi Kasei discovered the activity of lead compounds in catalyzing transesterification, stating that a variety of such compounds, including lead oxides, lead salts, alkyl lead, and alkoxy lead, serve as transesterification catalysts. Subsequently, researchers further investigated them.

Wang et al. [38] studied the activity of several Lewis acids and bases as catalysts for the transesterification. Among them, lead acetate trihydrate showed higher activity and selectivity. By optimizing the reaction conditions, under the catalysis of lead acetate trihydrate, the conversion of phenol could reach 24.8%, MPC selectivity was 76.5%, and DPC selectivity was 23.5%. Fukuoka et al. [41] compared the performance of organometallics of titanium, tin, and lead in catalyzing the reaction of DMC and PhOH in a reaction distillation column, as shown in Table 5. The organic salts of lead exhibited excellent catalytic performance, surpassing that of titanium salts and tin organometallics.

Table 5. Comparison of the activities of homogeneous Ti-, Sn-, and Pb-based catalysts (data from [41]).

| Catalyst | MPC | | DPC | |
|----------------------|-----------|-----------------|-----------|-----------------|
| | Yield (%) | Selectivity (%) | Yield (%) | Selectivity (%) |
| Ti(OPh) ₄ | 6.2 | 98.0 | 0.1 | 1.0 |
| Bu ₂ SnO | 7.9 | 98.0 | 0.1 | 1.0 |
| Pb(OPh) ₂ | 11.3 | 97.0 | 0.2 | 2.0 |

Although organic lead compounds exhibit higher catalytic performance than organic titanium and tin compounds, lead is highly toxic to humans, so they pose safety hazards in their use and have been phased out.

3.4. Rare-Earth-Metal-Based Catalysts

Mitsubishi Chemical first disclosed an example of using a rare-earth metal yttrium alkoxide compound as a homogeneous catalyst for catalyzing transesterification. Since then, a small number of rare-earth metal compounds used as catalysts have been reported. Rare-earth metals are used as catalysts primarily because of their Lewis acidic nature. Mei et al. [42] found that samarium trifluoromethanesulfonate exhibits transesterification activity and can exist stably in water and air, demonstrating good catalytic stability. Similarly, Wang et al. [43] studied samarium-based catalysts and found that diiodosamarium is a better catalyst, with a phenol conversion of 52.8% and MPC and DPC yields of 26.5% and 22.8%, respectively, higher in activity compared to titanium tetrabutoxide and dibutyltin oxide. The catalytic activity of rare-earth-metal-based catalysts is listed in Table 6.

Table 6. Activity of homogeneous rare-earth-metal-based catalysts.

| Catalyst | Temperature (°C) | Time (h) | PhOH/DMC | Cat/PhOH (in Mass) | Conversion ** (%) | MPC Yield (%) | DPC Yield (%) | Transesterification Selectivity (%) * | Ref. |
|----------------------|------------------|----------|----------|--------------------|-------------------|---------------|---------------|---------------------------------------|------|
| SmI ₂ | 150–180 | 8 | 1 | 0.002 | 47.7 | 26 | 18.7 | 93.7 | [43] |
| Sm(OTf) ₃ | 190 | 12 | 4 | 0.0036 | 34.4 *** | 2.1 | 31.1 | 96.5 | [42] |

* Transesterification selectivity includes both DPC and MPC. ** Conversion is calculated based on phenol unless stated otherwise. *** Conversion is calculated based on DMC.

4. Heterogeneous Catalysts for Transesterification

Homogeneous catalysts exhibit good catalytic activity; however, they inevitably face the challenge of catalyst separation. Utilizing non-homogeneous catalysts is one solution to this problem. Currently, heterogeneous catalysts for transesterification can be classified into four categories: oxides, molecular sieves, hydrotalcites, and heteropolyacids.

4.1. Oxides

4.1.1. TiO₂

Since the activity of homogeneous catalysts depends on the metal center, a natural strategy for heterogenization is to utilize the corresponding metal oxide. Titanium dioxide (TiO₂) is one such example. The activity of TiO₂-based heterogeneous catalysts reported in the literature is summarized in Table 7.

Table 7. Activity of heterogeneous TiO₂-based catalysts.

| Catalyst | Temperature (°C) | Time (h) | PhOH/DMC | Cat/PhOH (in Mass) | Conversion (%) | MPC Yield (%) | DPC Yield (%) | Transesterification Selectivity (%) * | Ref. |
|------------------------------------|------------------|----------|----------|--------------------|----------------|---------------|---------------|---------------------------------------|------|
| TiO ₂ | 150–180 | 9 | 1 | 0.013 | 29.5 | 8.9 | 20.4 | 99.7 | [44] |
| TiO ₂ /SiO ₂ | 430 | N.A.*** | 0.2 | N.A.*** | 37 | 31 | 0 | 87 | [45] |
| TiO ₂ -ZnO | 160–180 | 8 | 1 | 0.015 | 41.2 | 22.9 | 17.6 | 98.2 | [46] |
| TiO ₂ /CNT | 150–180 | 9 | 1 | 0.053 | 25.3 | 14.1 | 11.2 | 99.9 | [47] |
| TiO ₂ /CNT-S | 150–180 | 9 | 1 | 0.053 | 41.6 | 18.3 | 23.3 | 99.9 | [47] |
| TiO ₂ /CNT-C | 150–180 | 9 | 1 | 0.053 | 43.9 | 23.9 | 20 | 99.9 | [47] |
| TiO ₂ -C60-8 | 160–180 | 8 | 1 | 0.015 | 34.4 | 17.1 | 17.3 | 99.9 | [48] |
| TiO ₂ -RGO-50 | 150–180 | 9 | 1 | 0.013 | 53.5 | 17.6 | 35.8 | 99.9 | [49] |
| TiO ₂ @SiO ₂ | 150–180 | 9 | 1 | 0.013 | 41.8 | 17.7 | 24.1 | 100 | [50] |
| TiO ₂ -Nanotube | 170 | 10 | 0.056 | 0.106 | 54.6 | 10.1 | 44.1 | 99.2 | [44] |

* Transesterification selectivity includes both DPC and MPC. ** Conversion is calculated based on phenol unless stated otherwise. *** N.A.: Not Available.

Lee et al. [45] first proposed TiO₂ supported on SiO₂ as a catalyst for gas-phase transesterification. The catalytic activity results indicated that, due to thermodynamic limitations, anisole was predominantly produced. XPS and XANES spectra indicated the participation of Ti(IV) species on the catalyst surface in the transesterification, with rutile also serving as catalytically active sites but prone to deactivation by carbon deposition. To address the low DPC selectivity in gas-phase reactions, Lee et al. [51] proposed a two-step reaction strategy, employing a gas-phase reaction for MPC formation in the first step and a liquid-phase reaction for the subsequent disproportionation reaction.

To further enhance the catalytic activity of TiO₂, researchers made several improvements. Wang et al. [47] modified carbon nanotubes (CNTs) with the surfactants CTAB and SDS and loaded TiO₂ to prepare TiO₂/CNT catalysts for transesterification. The modified CNT support facilitated TiO₂ dispersion, contributing to the enhanced catalytic activity of TiO₂/CNT catalysts for transesterification, with a phenol conversion of 43.9%, similar to homogeneous catalysts. Since surfactants altered the surface charge of CNTs, stabilizing the Ti species, catalytic stability was also improved. Considering the preparation strategy chosen by the authors, as the Ti(OH)_n⁴⁻ⁿ species obtained from the hydrolysis of titanium alkoxides are negatively charged, the use of the cationic surfactant CTAB was advantageous, with only an 8% decrease in activity after four cycles of catalyst recycling. XPS and XRD spectra jointly indicated that amorphous TiO₂ was the active center for catalyzing transesterification.

Modifying the texture properties and morphology of catalysts can also promote transesterification. Wang et al. [50] prepared TiO₂@SiO₂ core-shell catalysts with TiO₂ as the core and SiO₂ as the shell, where the TiO₂ core thickness ranged from 220 to 300 nm and the SiO₂ shell thickness ranged from 4 to 60 nm. The Ti-O-Si bonds formed in the core-shell structure maintained the four-coordinated structure of amorphous TiO₂, promoting transesterification. Additionally, the core-shell structure inhibited the loss of TiO₂ species, with no decrease in activity after four cycles of catalyst reuse. Li et al. [44] synthesized TiO₂ nanotubes and compared them with anatase, finding that TiO₂ nanotubes exhibited better catalytic activity, with a phenol conversion of up to 54.6% at 170 °C and a selectivity of up to 99.2%. This was attributed to the larger specific surface area, pore size, and number of surface defects of nanotubes. The characterization of dimethyl carbonate adsorption and

activation on TiO₂ nanotube surfaces using DRIFT and TG-MS revealed the coexistence of three adsorption forms on TiO₂ nanotubes, as shown in Figure 9, with only adsorption form I related to transesterification, while forms II and III promoted the generation of anisole; nevertheless, these patterns all reflect the coordination of carbonyl in DMC and Ti Lewis acid sites in TiO₂. Furthermore, hydroxyl groups on the surface of TiO₂ nanotubes also facilitated dimethyl carbonate adsorption, thereby promoting the reaction.

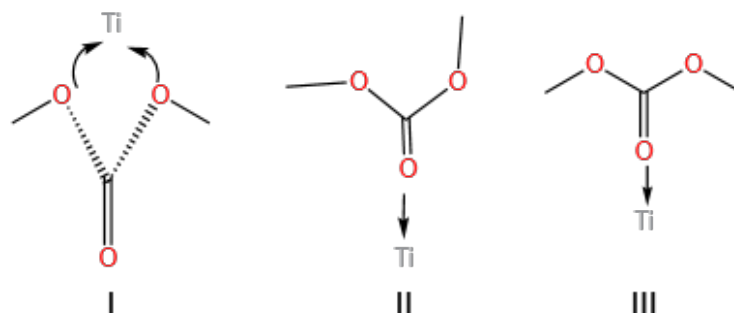


Figure 9. Three patterns of DMC adsorption on titania nanotubes (redrawn, data from [50]).

The chemical properties of TiO₂, such as electron cloud density and acidity, also have a significant impact on the activity of transesterification. Wang et al. [46] proposed the use of ZnO-modified TiO₂, where amorphous TiO₂ served as the active center and amorphous ZnO acted as a promoter. Additionally, the loading amount of Zn and the calcination temperature of the catalyst significantly affected the acidity and acid strength of the catalyst. NH₃-TPD results indicated that weak acidic sites on the surface promoted the generation of MPC and DPC, while strong acidic sites promoted the formation of anisole as a byproduct. The catalyst 5TiZn-250, with a Ti/Zn ratio of 5 and a calcination temperature of 250 °C, exhibited the optimal activity, with phenol conversion and transesterification selectivity reaching 41.2% and 98.2%, respectively, whereas the phenol conversion of unmodified TiO₂ was only 15%. Furthermore, the 5TiZn-250 catalyst retained its activity with a slight decrease after three repeated uses, attributed to the phase transformation of composite oxides and the loss of Ti species.

C60 is a commonly used electron modulation additive that has been shown to have significant effects on Cu-based catalysts. Wang et al. [48] also proposed C60-modified TiO₂, which promoted the dispersion of TiO₂, and the electron density of the Ti species on it could be adjusted by changing the preparation conditions and the ratio of C60 to Ti. XPS results showed that C60 reduced the electron cloud density on TiO₂, enhancing its Lewis acidity and thereby promoting the reaction activity. It is noteworthy that the TiO₂/C60 catalyst exhibited excellent selectivity for DPC, with a molar ratio of Ti to C60 of 8:1, and at a calcination temperature of 200 °C, the phenol conversion of C60-TiO₂-8 was 36.5%, and DPC selectivity was 86.5%, much higher than the 50% obtained with the Ti-based catalyst, attributed to the electronic effect of C60, the effective dispersion of C60 on the Ti species, and the synergistic effect between C60 and TiO₂. After continuous operation for four cycles, the phenol conversion gradually decreased due to the loss of Ti species. Wang et al. [49] also employed another carbon material, reduced graphene oxide (RGO), to modify the electronic properties of TiO₂. The results showed that, similar to C60, RGO significantly improved the dispersion and chemical state of TiO₂, leading to an increase in Lewis acid sites of TiO₂, thereby promoting transesterification. The TiO₂-rGO composite material containing 50% rGO achieved a phenol conversion of 53.5% and a transesterification selectivity of 99.9% under optimized conditions, comparable to homogeneous catalysts.

4.1.2. Lead Oxides

Similar to their corresponding homogeneous catalysts, lead oxides have also been used in transesterification. Current research on Pb oxide catalysts mainly focuses on bimetallic

composite oxides, with an emphasis on the modulation effect of the second metal on Pb. The activity of Pb-based heterogeneous catalysts is shown in Table 8.

Table 8. Activity of heterogeneous lead-based catalysts.

| Catalyst | Temperature (°C) | Time (h) | PhOH/DMC | Cat/PhOH (in Mass) | Conversion (%) | MPC Yield (%) | DPC Yield (%) | Transesterification Selectivity * (%) | Ref. |
|---|------------------|-------------|----------|--------------------|----------------|---------------|---------------|---------------------------------------|---------|
| PbO | 180 | 8–10 | 0.82 | 0.06 | 22.0 | 7.6 | 14.4 | 100 | [52] |
| O ₂ -PbO/MgO | 180 | 8–10 | 0.82 | 0.06 | 36.8 | 10.0 | 26.6 | 99.5 | [53] |
| PbO-ZnO | 180 | N.A. *** | 0.8 | 0.02 | 64.6 | N.D. | 45.6 | 72 | [52] |
| 15.2PbZr *** | 200 | 2.5 | N.A. *** | 0.053 | 76.6 | N.A. | 76.1 | 99.3 | [54,55] |
| 15.2PbTi *** | 200 | 2.5 | N.A. *** | 0.053 | 34.2 | N.A. | 32.9 | 96.2 | [54] |
| 15.2PbAl *** | 200 | 2.5 | N.A. *** | 0.053 | 47.3 | N.A. | 43.1 | 91.1 | [54] |
| 15.2PbSi *** | 200 | 2.5 | N.A. *** | 0.053 | 56.6 | N.A. | 55.1 | 97.3 | [54] |
| 15.2PbMg *** | 200 | 2.5 | N.A. *** | 0.053 | 67.5 | N.A. | 62.1 | 92 | [54] |
| PbO-ZnO | 160 | 10 | 2 | 0.04 | 32.0 **** | 28.0 | 2.5 | 95.3 | [56] |
| PbO-Fe ₂ O ₃ | 160 | 10 | 2 | 0.04 | 33.7 **** | 31.7 | 2.0 | 100.0 | [56] |
| PbO-La ₂ O ₃ | 160 | 10 | 2 | 0.04 | 50.0 **** | 39.6 | 4.7 | 88.6 | [56] |
| PbO-NiO | 160 | 10 | 2 | 0.04 | 61.1 **** | 37.4 | 11.8 | 80.5 | [56] |
| PbO-ZrO ₂ | 160 | 10 | 2 | 0.04 | 22.7 **** | 21.7 | 0 | 95.6 | [56] |
| PbO-Ce ₂ O ₃ | 160 | 10 | 2 | 0.04 | 62.2 **** | 51.7 | 7.2 | 94.7 | [56] |
| PbO-Sm ₂ O ₃ | 160 | 10 | 2 | 0.04 | 62.0 **** | 36.2 | 13.8 | 80.6 | [56] |
| PbO-Y ₂ O ₃ | 160 | 10 | 2 | 0.04 | 47.2 **** | 36.9 | 5.2 | 89.2 | [56] |
| PbO-Yb ₂ O ₃ | 160 | 10 | 2 | 0.04 | 57.5 **** | 39.7 | 11.0 | 88.2 | [56] |
| PbO/MgO ***** | 200 | 2.5 | N.A. | 0.053 | 60.1 | N.A. | 56.0 | 93.2 | [57] |
| PbO/ZrO ₂ ***** | 200 | 2.5 | N.A. | 0.053 | 56.3 | N.A. | 55.2 | 98.0 | [57] |
| PbO/SiO ₂ ***** | 200 | 2.5 | N.A. | 0.053 | 47.7 | N.A. | 46.2 | 96.9 | [57] |
| PbO/Al ₂ O ₃ ***** | 200 | 2.5 | N.A. | 0.053 | 30.2 | N.A. | 26.5 | 87.7 | [57] |
| PbO/TiO ₂ ***** | 200 | 2.5 | N.A. | 0.053 | 24.3 | N.A. | 22.9 | 94.2 | [57] |
| PbTiO ₃ ***** | 180 | 9 | 2 | N.A. | 27.8 | 16.3 | 9.2 | 91.7 | [58] |

* Transesterification selectivity includes both DPC and MPC. ** Conversion is calculated based on phenol unless stated otherwise. *** N.A. Not Available. * N.D. Not Detected. **** Conversion is calculated based on DMC. ***** MPC disproportionation.

Wang et al. [52] prepared a Pb-Zn composite oxide for transesterification. The influence of the preparation method, calcination temperature, precursor, and Pb/Zn molar ratio on the catalytic activity was studied. The results indicated that Pb₃O₄ was the primary active phase, while amorphous ZnO primarily served as a promoter. Under the conditions of a calcination temperature of 500 ° and a Pb/Zn ratio of 2:1, the catalyst achieved the highest activity, with a DPC yield of 45.6%. The deactivation of the catalyst was attributed to the transformation of Pb₃O₄ into PbO. To address the deactivation issue, further studies were conducted [59], revealing that phenol in the catalyst reacted with lead to form Pb₄O(OPh)₆, resulting in a crystalline phase transformation of the active component and subsequent loss, leading to catalyst deactivation.

Some researchers have also considered PbO as the active phase. Meng et al. [53] screened PbO catalysts loaded on different supports, and the results showed that magnesium oxide was optimal. Moreover, the activity of PbO/MgO catalysts could be further enhanced by oxidative modification, with yields of MPC and DPC reaching 10% and 26.6%, respectively. Mechanistic analysis indicated that, after promotion by O₂, the structure and oxidation state of lead in PbO/MgO catalysts changed, leading to the presence of strong PbO-MgO interactions. Hu et al. [56] selected yttrium oxide as the preferred support for transesterification and optimized the reaction conditions through orthogonal experiments. The results showed that a catalyst with a Pb:Y molar ratio of 2:1 and calcination at 700 °C exhibited good reaction performance, with a DMC conversion of 56.87%, DPC yield of 17.10%, MPC yield of 33.24%, and anisole yield of 6.53%. The catalyst maintained good activity after multiple recycles.

Wang et al. [54,55] prepared PbO-ZrO₂ catalysts (PbZr) using a coprecipitation method. The PbZr catalyst with a PbO loading of 15.2 wt% (15.2PbZr) exhibited optimal catalytic performance. Under the best conditions (200 °C, 2.5 h, 1.2 g catalyst), the MPC conversion reached 76.6%, and the DPC selectivity was 99.3%. This was attributed to the strongest interaction between Pb and Zr, the highest dispersion of PbO, and the largest surface area and pore volume. Repetitive experiments showed that 15.2PbZr could be reused five times without deactivation, and the DPC selectivity remained at 99.0%, with no loss of Pb species. This was due to the favorable interaction between Pb and Zr and the partial incorporation of Pb into the ZrO₂ structure. Furthermore, they conducted further research on the role of crystalline ZrO₂ and prepared PbO supported on ZrO₂ with pure tetragonal/monoclinic crystal phases [60]. The results showed that tetragonal zirconia was a better support with a higher surface area and Lewis acidity, resulting in higher catalytic activity and selectivity.

Wang et al. [57] further optimized the support type for MPC disproportionation, preparing a series of Pb-based catalysts on MgO, ZrO₂, SiO₂, TiO₂, and Al₂O₃. The results showed that the dispersion of Pb on SiO₂, TiO₂, ZrO₂, and MgO was superior to that on Al₂O₃, and stronger metal-carrier interactions were observed on MgO and ZrO₂. The activity results indicated that PbO/MgO and PbO/ZrO₂ exhibited higher catalytic activity due to their higher Pb dispersion and greater number of Lewis acid sites. Owing to the strong interaction between highly dispersed Pb and the carrier, PbO/MgO and PbO/ZrO₂ showed better reusability. In contrast, the decrease in activity observed for PbO/SiO₂, PbO/Al₂O₃, and PbO/TiO₂ was mainly attributed to Pb loss.

In addition to composite oxides, lead can also be embedded into the lattice of perovskite to form Lewis acid sites for transesterification. For example, Li et al. [58] prepared lead titanate pyrochlore through a hydrothermal method for transesterification and adjusted its crystal structure by varying the calcination temperature. Lead titanate calcined at 500 °C exhibited a perovskite-type PbTiO₃ structure, showing the best catalytic activity, with a DMC conversion rate of 27.8% and MPC and DPC yields of 16.3% and 9.2%, respectively.

4.1.3. Molybdenum Oxides

Mo-based catalysts are effective for transesterification, such as the transesterification of dimethyl oxalate with phenol. Therefore, Mo-based catalysts have also been used for the transesterification of dimethyl carbonate with phenol. The activity of heterogeneous Mo-based catalysts reported in the literature is listed in Table 9.

Table 9. Activity of heterogeneous molybdenum-based catalysts.

| Catalyst | Temperature (°C) | Time (h) | PhOH/DMC | Cat/PhOH (in Mass) | Conversion (%) | MPC Yield (%) | DPC Yield (%) | Transesterification Selectivity* (%) | Ref. |
|--|------------------|----------|----------|--------------------|----------------|---------------|---------------|--------------------------------------|------|
| MoO ₃ | 160 | 4 | 0.2 | 0.09 | 3.8 | 3.8 | N.D.*** | 100 | [61] |
| MoO ₃ /SiO ₂ | 160 | 4 | 0.2 | 0.09 | 17.3 | 17.1 | 0.2 | 100 | [61] |
| MoO ₃ /FSM-36 | 160 | 4 | 0.2 | 0.09 | 14.7 | 14.3 | 0.1 | 97.3 | [61] |
| MoO ₃ /ZrO ₂ | 160 | 4 | 0.2 | 0.09 | 13.9 | 13.5 | 0.1 | 97.1 | [61] |
| MoO ₃ /TiO ₂ | 160 | 4 | 0.2 | 0.09 | 9.3 | 8.9 | 0.0 | 95.7 | [61] |
| MoO ₃ /SiO ₂ -Al ₂ O ₃ | 160 | 4 | 0.2 | 0.09 | 18.3 | 4.3 | 0.0 | 23.5 | [61] |
| MoO ₃ /Al ₂ O ₃ | 160 | 4 | 0.2 | 0.09 | 20.0 | 3.6 | 0.0 | 18 | [61] |
| MoO ₃ /CaO | 160 | 4 | 0.2 | 0.09 | 23.2 | 2.0 | 0.0 | 8.6 | [61] |
| Mo-K | 150–180 | 9 | 1 | 0.048 | 15.6 | 15.7 | 15.3 | 92.9 | [62] |
| Mo-Mg | 150–180 | 9 | 1 | 0.048 | 17.9 | 6.7 | 7.8 | 90.5 | [62] |
| Mo-Pb | 150–180 | 9 | 1 | 0.048 | 17.1 | 9.1 | 7.1 | 93.0 | [62] |
| Mo-Bi | 150–180 | 9 | 1 | 0.048 | 14.2 | 9.3 | 6.6 | 97.9 | [62] |
| Mo-Co | 150–180 | 9 | 1 | 0.048 | 21.4 | 5.4 | 8.5 | 96.3 | [62] |
| Mo-Zn | 150–180 | 9 | 1 | 0.048 | 24.2 | 9.7 | 10.9 | 96.3 | [62] |
| Mo-Cr | 150–180 | 9 | 1 | 0.048 | 25.3 | 11.4 | 11.9 | 97.6 | [62] |
| Mo-Sb | 150–180 | 9 | 1 | 0.048 | 32.7 | 10.2 | 14.5 | 97.2 | [62] |
| Mo-Cu | 150–180 | 9 | 1 | 0.048 | 41.6 | 14.0 | 17.8 | 93.3 | [62] |

* Transesterification selectivity includes both DPC and MPC. ** Conversion is calculated based on phenol unless stated otherwise. *** N.D. Not Detected.

Ono et al. [61] first reported the catalytic activity of unsupported MoO_3 in transesterification, with a DPC yield of only 3.8%. However, when MoO_3 was loaded onto SiO_2 , the DPC yield increased to 17%. The authors also proposed the mechanism of transesterification on $\text{MoO}_3/\text{SiO}_2$ shown in Figure 10, where phenol dissociates and adsorbs onto the surface of molybdenum, followed by interaction between DMC molecules and adsorbed phenol to form transesterification products.

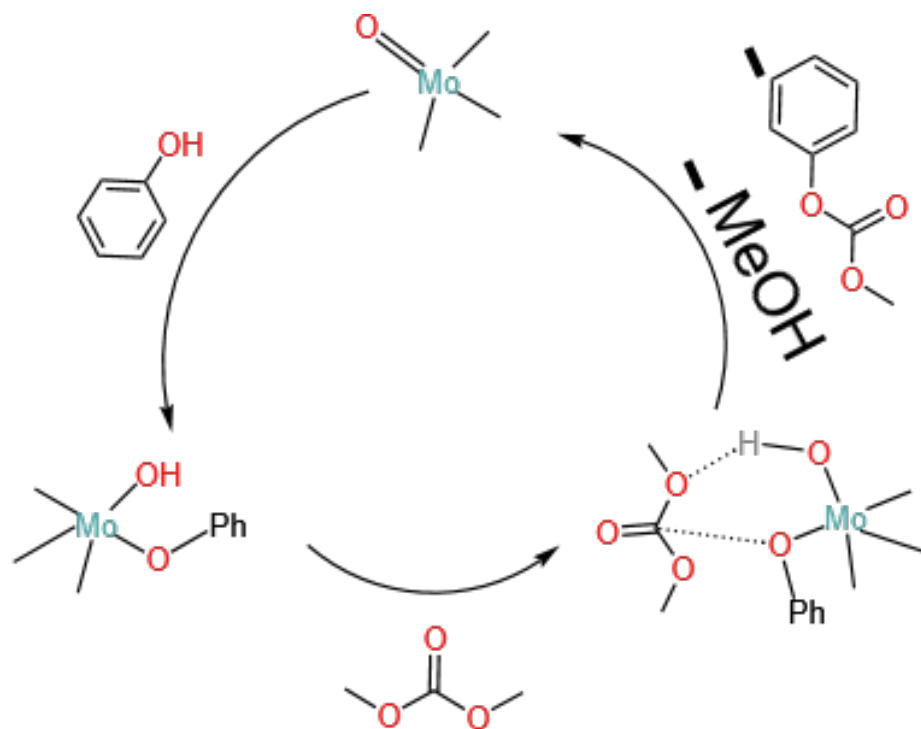


Figure 10. Mechanism of transesterification on MoO_3 catalysts (redrawn, data from [61]).

Subsequent work focused on the development of supported MoO_3 catalysts. Wang et al. [63] prepared $\text{MoO}_3/\text{SiO}_2$ catalysts using different methods for MPC disproportionation. The results showed that $\text{MoO}_3/\text{SiO}_2$ prepared by combining sol-gel and hydrothermal treatment (M-SGH) exhibited higher catalytic activity, with MoO_3 having a higher dispersion, a larger specific surface area, and larger pores. Under optimal conditions, the conversion of MPC reached 72.8%, and the yield of DPC was 71.4%. Additionally, M-SGH showed excellent reusability and regeneration. After seven consecutive runs, the MPC conversion decreased slightly from 72.8% to 56%, with carbon deposition being the main cause of catalyst deactivation. Deactivated M-SGH could be regenerated by calcination in air at 500 °C, and the catalyst activity was fully restored after regeneration. Li et al. [64] optimized the SiO_2 support and prepared SBA-16/ α - MoO_3 catalysts using a hydrothermal coprecipitation method with mesoporous silica SBA-16 as the support. Compared to α - MoO_3 and α - $\text{MoO}_3/\text{SBA-16}$ prepared by impregnation, SBA-16/ α - MoO_3 showed good catalytic activity in transesterification. At atmospheric pressure and a reaction temperature of 180 °C, the conversion of dimethyl carbonate reached 78.5%, and the selectivity of diphenyl carbonate was above 46.5%. The study showed that SBA-16/ α - MoO_3 effectively regulated the Si distribution on the surface of SBA-16, playing a key role in reducing carbon deposition and increasing the reaction rate. Addressing the deactivation issue of MoO_3 catalysts, Park et al. conducted further research. Temperature-programmed desorption profiles showed that reactants strongly adsorbed on the $\text{MoO}_3/\text{SiO}_2$ surface, leading to carbon deposition during the reaction process and subsequent deactivation. Carbon deposition could be partially removed by calcination in air at 550 °C. Small amounts of Mo species dissolved and leached into the reaction system during the reaction process, and these Mo species also exhibited catalytic activity.

In addition to controlling the properties of the support, additives can also be used to regulate the activity of Mo-based catalysts. Wang et al. [62] modified MoO₃ with Cu and found that a Mo/Cu molar ratio of 1:1 and a phenol/DMC molar ratio of 1:1 resulted in a phenol conversion of 49.9% and a total yield of MPC and DPC of 45.4%. Compared to bare MoO₃ catalysts, the activity was significantly improved. Repetitive experiments showed a gradual decrease in activity after repeated use of the catalyst, possibly due to the leaching of molybdenum and copper and carbon deposition.

4.1.4. Other Oxides or Hydroxides

There are several reports on other types of oxides, and the results are summarized in Table 10.

Table 10. Activity of heterogeneous molybdenum-based catalysts.

| Catalyst | Temperature (°C) | Time (h) | PhOH/DMC | Cat/PhOH (in Mass) | Conversion ** (%) | MPC Yield (%) | DPC Yield (%) | Transesterification Selectivity * (%) | Ref. |
|---|------------------|----------|----------|--------------------|-------------------|---------------|---------------|---------------------------------------|------|
| Nanosheet-MgO | 180 | 13 | 2 | 0.002 **** | N.A. *** | N.A. *** | N.A. *** | 95.7 | [65] |
| Flake-Mg(OH) ₂ | 180 | 13 | 2 | 0.002 **** | 25.9 | 6.1 | 17.8 | 92.3 | [66] |
| V ₂ O ₅ | 150–180 | 9 | 1.5 | 0.016 **** | 42.0 | 17.5 | 22.6 | 95.5 | [67] |
| V-Cu | 150–180 | 9 | 1 | 0.013 **** | 37.0 | 20.2 | 15.6 | 96.8 | [68] |
| V ₂ O ₅ -HCl | 180 | 13 | 2 | 0.0025 **** | 23.23 ***** | 0.93 | 12.94 | 100.0 | [69] |
| V ₂ O ₅ -NHO ₃ | 180 | 13 | 2 | 0.0025 **** | 6.81 | 2.49 | 20.95 | 100.0 | [69] |
| V ₂ O ₅ -H ₂ SO ₄ | 180 | 13 | 2 | 0.0025 **** | 15.4 | 5.58 | 1.15 | 98.7 | [69] |
| V ₂ O ₅ -H ₃ PW ₁₂ O ₄₀ | 180 | 13 | 2 | 0.0025 **** | 50.64 | 2.64 | 12.73 | 99.5 | [69] |
| V ₂ O ₅ -H ₄ SiW ₁₂ O ₄₀ | 180 | 13 | 2 | 0.0025 **** | 1.71 | 0.34 | 0.29 | 97.5 | [69] |
| V ₂ O ₅ /SiO ₂ | 180 | 12 | 10 | 0.053 | 42.4 | 16.7 | 25.7 | 100.0 | [70] |

* Transesterification selectivity includes both DPC and MPC. ** Conversion is calculated based on phenol unless stated otherwise. *** N.A. Not Available. **** Calculated on mole basis. ***** Conversion is calculated based on DMC.

Some alkaline oxides can also catalyze transesterification, with MgO being a representative. Wang et al. [65] evaluated the activity of MgO nanosheets in transesterification. The results showed that under the conditions of 180 °C, a molar ratio of phenol to dimethyl carbonate of 2:1, a reaction time of 13 h, and a catalyst loading of 0.2% (with respect to phenol), the selectivity of transesterification reached 95.7%. Furthermore, the reacted MgO nanosheets could be regenerated by vacuum calcination, and the activity was completely restored after regeneration. Similarly, Hu et al. [66] prepared hexagonal Mg(OH)₂ flakes by a polyethylene glycol-assisted hydrothermal synthesis method for transesterification. The morphological characteristics of the nanoflakes further enhanced the catalytic activity and led to higher stability compared to catalysts without this specific morphology. The deactivated hexagonal Mg(OH)₂ flakes could be easily regenerated by calcination under vacuum, showing good reusability.

Other reported oxide catalysts include vanadium-based oxides. Wang et al. [67] first reported the application of V₂O₅ in transesterification. V₂O₅ was directly prepared by calcining ammonium metavanadate. Under the conditions of a catalyst mass fraction of 1.6%, a DMC/phenol molar ratio of 1.5:1, and a reaction time of 9 h, the maximum conversion of phenol was 42.0%, with a total yield of 40.1%. Repetitive experiments showed the significant deactivation of the catalyst, mainly due to the phase transition of V₂O₅ to V₄O₉ and carbon deposition, with the reduction of V₂O₅ by some reactants being a major factor in the phase transition. The activity of the deactivated catalyst could be partially restored after calcination in air. Subsequently, they modified V₂O₅ with Cu [68] and found that the catalyst exhibited the highest activity when the V:Cu molar ratio was 4:1. Under the conditions of 150–180 °C and 9 h, the conversion of phenol and the selectivity of the transesterification were 37.0% and 96.8%, respectively. The crystal phases of the V-Cu composite oxide were V₂O₅ and CuV₂O₆, both of which were active phases. Repetitive experiments showed that the V-Cu composite oxide continued to

deactivate, and after three repeated uses, the catalyst activity decreased from 37.0% to 23.7%. Subsequently, Hu et al. [69] further explored the effects of V_2O_5 microstructure and its catalytic mechanism. Ammonium metavanadate was acid-washed as a precursor and then calcined in air to obtain V_2O_5 . Pre-treatment of the precursor with hydrochloric acid and subsequent reaction under the conditions of 180 °C, a catalyst dosage of 0.2% (with respect to phenol), a DMC/phenol molar ratio of 1:2, and a reaction time of 13 h resulted in a maximum conversion of DMC of 23.23% and a selectivity for the transesterification close to 100%. They proposed the reaction mechanism on V_2O_5 shown in Figure 11, where the carbonyl group initially coordinates to V(V), followed by an attack by PhO^- to form MPC, and the carbonyl group of MPC is attacked again after coordinating with V(V) to form DPC, or it is attacked by a second MPC to undergo disproportionation to DPC.

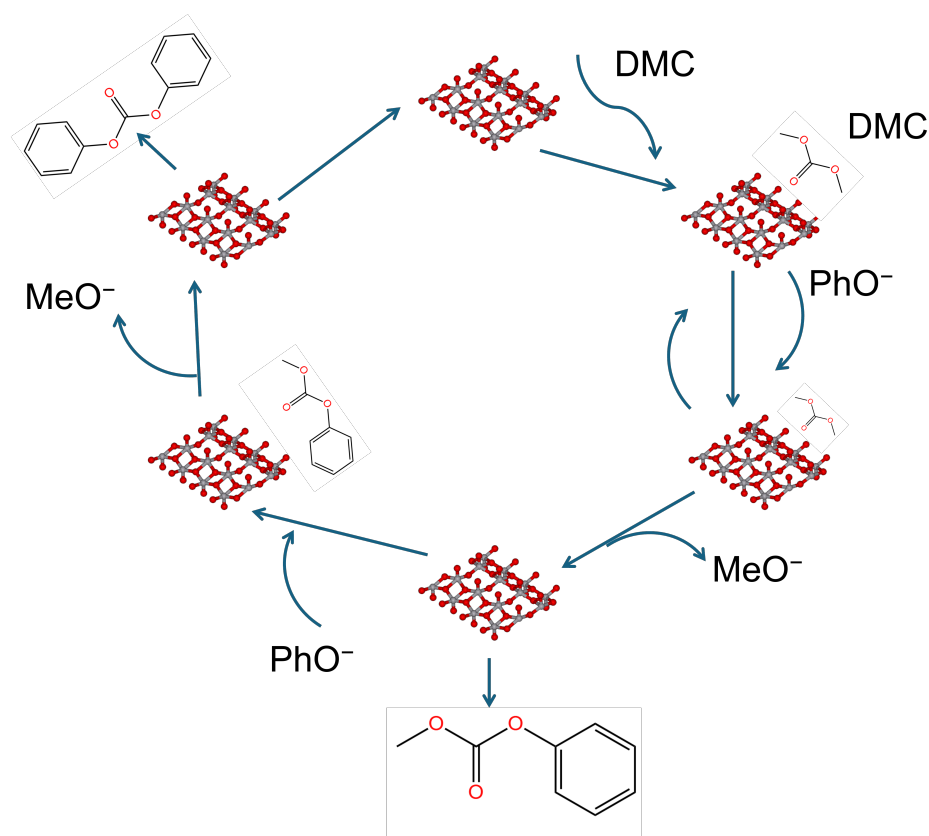


Figure 11. Mechanism of transesterification on V_2O_5 catalysts (redrawn, data from [69]).

In order to avoid the mass transfer limitation of transesterification caused by the catalyst surface area, Wang et al. [70] further loaded V_2O_5 onto a support and studied the relationship between catalyst porosity and transesterification activity. The results showed that a microporous support such as zeolite tended to generate anisole, while the mesoporous catalyst was more favorable for transesterification. The V_2O_5/SiO_2 catalyst supported on mesoporous SiO_2 obtained the best activity with a V_2O_5 loading of 40% (mass fraction); the selectivity of DPC was 60.6%, while the yield of DPC was 25.7%.

4.2. Molecular Sieves

Molecular sieves, including zeotypes and mesoporous silica, are materials composed of silicon, aluminum, and other heteroatoms with ordered porosity [71,72]. Adjusting the metal sites on molecular sieves can impart Lewis acidity, such as non-framework aluminum in HZSM-5 and framework titanium in TS-1 zeolites [73,74]. Therefore, utilizing molecular sieves as catalysts for transesterification is feasible. The catalytic activities of molecular-sieve-based catalysts reported in the literature are summarized in Table 11.

Table 11. Activity of heterogeneous molecular sieve-based catalysts.

| Catalyst | Temperature (°C) | Time (h) | PhOH/DMC | Cat/PhOH (in Mass) | Conversion ** (%) | MPC Yield (%) | DPC Yield (%) | Transesterification Selectivity * (%) | Ref. |
|---------------------------|------------------|----------|----------|--------------------|-------------------|---------------|---------------|---------------------------------------|------|
| Ti-Beta | 150–180 | 10 | 1 | 0.106 | 20.22 | 8.24 | 2.53 | 53.2 | [75] |
| Mo-HMS | 150–180 | 9 | 1 | 0.066 | 5.6 | 4.4 | 0.8 | 92.5 | [76] |
| Sn-HMS | 150–180 | 9 | 1 | 0.066 | 5.3 | 4.3 | 0.6 | 91.9 | [76] |
| Al-HMS | 150–180 | 9 | 1 | 0.066 | 14.6 | 2.1 | 1.4 | 23.4 | [76] |
| Ti-HMS | 150–180 | 9 | 1 | 0.066 | 31.4 | 14.6 | 16.8 | 99.9 | [76] |
| 10%V-20%Ti-MCM-41 | 180 | 8 | 1 | 0.017 | 33.88 *** | 21.47 | 12.41 | 100 | [77] |
| Sn-SiO ₂ | 160–180 | 9 | 1 | 0.033 | 29.4 | 14.7 | 14.7 | 99.9 | [78] |
| Sn-MSiO ₂ | 160–180 | 9 | 1 | 0.033 | 41.2 | 24.3 | 16.9 | 99.9 | [78] |
| Sn-MSiO ₂ -Cal | 160–180 | 9 | 1 | 0.033 | 34.7 | 19.4 | 15.3 | 99.9 | [78] |

* Transesterification selectivity includes both DPC and MPC. ** Conversion is calculated based on phenol unless stated otherwise. *** Conversion is calculated based on DMC.

Qiu et al. [75] employed the gas-phase substitution method to prepare Ti-Beta zeolite for transesterification. The results indicate that Ti-Beta zeolite exhibits excellent catalytic activity. When compared with TiO₂ and H-Beta zeolite, it was found that the framework Ti sites on Ti-Beta zeolite are the active centers for transesterification. After 10 h of reaction at 175 °C, the total yield of methyl phenyl carbonate (MPC) and diphenyl carbonate (DPC) can reach 10.77%, higher than the 2.38% achieved with TiO₂. Wang et al. [76] expanded the application to mesoporous molecular sieves, preparing a series of metal (Mo, Sn, Al, and Ti)-doped HMS mesoporous molecular sieves via hydrothermal synthesis for transesterification. It was found that Ti-HMS exhibited the best catalytic activity. When the molar ratio of Ti/Si reached 1/30, the Ti species inside the framework of Ti-HMS approached saturation, with a maximum phenol conversion of 31.4% and a transesterification selectivity of 99.9%. Shen et al. [77] prepared V₂O₅-Ti-MCM-41 catalysts, where V species served as a dopant to further enhance the catalytic activity of Ti-MCM-41. With the 10%V-20%Ti-MCM-41 catalyst, the optimal catalytic activity was achieved with a DMC conversion of 33.88%, a DPC selectivity of 35.84%, and a DPC yield of 12.14%.

Molecular sieves can also serve as supports for Lewis acid immobilization. Wang et al. [78] used SnCl₄ as the tin source to prepare organotin silanes, which were grafted into the channels of SBA-15 mesoporous molecular sieves. By using different template removal methods (extraction and calcination), they varied the surface silanol content of SBA-15 and investigated its effect on the grafted tin species. The results showed that the surface silanol affected the loading of organotin catalysts, with a higher surface silanol content resulting in a higher tin loading and better activity. At 160–180 °C for 9 h with a catalyst dosage of 1.0 g, the phenol conversion reached 50.4%, with transesterification selectivity exceeding 99.9%. Compared with literature reports, this study's method of organotin immobilization is simpler, with a higher tin loading, and the catalyst contains more T2 and T3 species, conducive to the stability of organotin immobilization.

4.3. Hydrotalcite

Hydrotalcite is a material with an interlayer structure. This layered material is composed of positively charged layers and anions with balanced charges. The interaction forces between the anions in the middle and between the layers are weak, and the cations are typically exchangeable. This results in its adjustable acidity, basicity, and redox properties, laying a good foundation for its catalytic functionality. There have been reports on hydrotalcite catalyzing transesterification, summarized in Table 12.

Table 12. Activity of heterogeneous hydrotalcite-based catalysts.

| Catalyst | Temperature (°C) | Time (h) | PhOH/DMC | Cat/PhOH (in Mass) | Conversion** (%) | MPC Yield (%) | DPC Yield (%) | Transesterification Selectivity * (%) | Ref. |
|--------------|------------------|----------|----------|--------------------|------------------|---------------|---------------|---------------------------------------|------|
| Mg-Al-HT | 160–180 | 10 | 2 | 0.015 | 31.9 | 14.7 | 11.6 | 82.4 | [79] |
| Mg-Al-HT-Cal | 160–180 | 10 | 2 | 0.015 | 15.0 | 7.5 | 1.3 | 58.7 | [79] |
| Zn-Al-HT-3 | 150–180 | 8 | 2 | 0.015 | 52.6 | 12.6 | 37.0 | 94.3 | [80] |
| MgAl | 150–180 | 8 | 2 | 0.01 | 51.8 | | 48.8 *** | 94.2 | [81] |
| ZnAl | 150–180 | 8 | 2 | 0.01 | 57.7 | | 53.1 *** | 92.0 | [81] |
| ZnFe | 150–180 | 8 | 2 | 0.01 | 35.4 | | 31.9 *** | 90.1 | [81] |
| NiFe | 150–180 | 8 | 2 | 0.01 | 37.6 | | 31.3 *** | 83.2 | [81] |
| ZnCr | 150–180 | 8 | 2 | 0.01 | 11.8 | | 11.8 *** | 100 | [81] |

* Transesterification selectivity includes both DPC and MPC. ** Conversion is calculated based on phenol unless stated otherwise. *** Total yield of DPC and MPC.

Li et al. [79] first proposed the use of hydrotalcite as a catalyst for transesterification. They studied the transesterification activity of hydrotalcites with different Mg/Al ratios and compared them with oxide catalysts. The results showed that Mg-Al hydrotalcite with a Mg/Al ratio of 2 exhibited the highest catalytic activity, surpassing oxide catalysts such as TiO₂/SiO₂, MoO₃/SiO₂, and Sm₂O₃. When DMC/PhOH = 2, the reaction time was 10 h, and the temperature was 160–180 °C, the total yield and selectivity of the transesterification were 26.3% and 82.4%, respectively, with a yield of 5.6% for diphenyl ether. To further modulate the catalytic activity, they attempted to use Zn-Al hydrotalcite as a catalyst [80]. The results showed that with Zn/Al = 3, PhOH/DMC = 2, a reaction temperature of 150–180 °C, and a reaction time of 12 h, the conversion of DMC reached 55.9%, with yields of 25.3% for DPC and 27% for MPC, and a selectivity of 93.6% for transesterification products. The calcination of Zn-Al hydrotalcite resulted in the disappearance of the layered structure and a significant decrease in catalytic activity. Considering that the calcined material exhibited higher alkalinity and a larger surface area than the parent hydrotalcite, the reason for the good catalytic activity of Zn-Al hydrotalcite may be due not only to its suitable alkalinity but also to its unique layered structure.

To further clarify the structure–activity relationship of metal ions on hydrotalcite in transesterification, Li et al. [81] studied the catalytic activity of five types of layered double hydroxide-like compounds (HTLCs) with different cation combinations (MgAl, ZnAl, ZnFe, NiFe, and ZnCr). The results showed that the catalytic performance of HTLCs was related to the nature of the involved cations. Trivalent cations affected the catalyst activity, while divalent cations influenced the stability. Trivalent cations influenced the Lewis acidity of the layer surface, thereby affecting the activity of transesterification, while divalent cations affected the stability of the octahedral coordination structure on the layer, thus affecting the intrinsic stability of the HTLC material. The analysis of deactivated catalysts revealed that the collapse of the HTLC layer structure was the cause of deactivation. MgAl hydrotalcite exhibited the best catalytic activity, with a conversion of DMC reaching 51.8% and a selectivity of 94.2% for DPC and MPC, with no change in catalytic activity after five uses.

4.4. Heteropolyacids and Heteropolyacid Salts

Heteropolyacids are also a common type of solid acid, composed of high-oxidation-state transition metal ions (V, Mo, W, etc.) coordinated by oxygen atoms to form a structure with the general formula [X_xM_mO_y]^{q-}, where M is the coordinating atom (e.g., V, Mo, or W), and X is a heteroatom (e.g., Si, P, or As). The catalytic activity of heteropolyacids or heteropolyacid salts reported in the literature is summarized in Table 13.

Table 13. Activity of heterogeneous heteropolymetalate-based catalysts.

| Catalyst | Temperature (°C) | Time (h) | PhOH/DMC | Cat/PhOH (in Mass) | Conversion (%) | ** MPC Yield (%) | DPC Yield (%) | Transesterification Selectivity * (%) | Ref. |
|---|------------------|----------|----------|--------------------|----------------|------------------|---------------|---------------------------------------|----------|
| KPMo | 150–180 | 8 | 1 | 0.004 **** | 1.0 | 1.0 | N.D. *** | 99.9 | [82] |
| H0.5CsPMo | 150–180 | 8 | 1 | 0.004 **** | 12.5 | 10.8 | 1.7 | 99.9 | [82] |
| LiPMo | 150–180 | 8 | 1 | 0.004 **** | 20.4 | 10.6 | 9.8 | 99.9 | [82] |
| NaPMo | 150–180 | 8 | 1 | 0.004 **** | 23.0 | 13.2 | 9.8 | 99.9 | [82] |
| MgPMo | 150–180 | 8 | 1 | 0.004 **** | 12.5 | 5.4 | 6.3 | 93.6 | [82] |
| CaPMo | 150–180 | 8 | 1 | 0.004 **** | 11.0 | 2.5 | 8.2 | 97.3 | [82] |
| BaPMo | 150–180 | 8 | 1 | 0.004 **** | 7.1 | 5.4 | 1.7 | 99.9 | [82] |
| PbPMo | 150–180 | 8 | 1 | 0.004 **** | 17.9 | 10.7 | 6.4 | 95.5 | [82] |
| AlPMo | 150–180 | 8 | 1 | 0.004 **** | 30.6 | 7.0 | 6.5 | 44.1 | [82] |
| CuPMo | 150–180 | 8 | 1 | 0.004 **** | 26.2 | 13.2 | 13.0 | 99.9 | [82] |
| ZnPMo | 150–180 | 8 | 1 | 0.004 **** | 28.2 | 13.8 | 13.0 | 95.0 | [82] |
| MnPMo | 150–180 | 8 | 1 | 0.004 **** | 10.3 | 3.7 | 6.3 | 97.1 | [82] |
| AgPMo | 150–180 | 8 | 1 | 0.004 **** | 17.6 | 8.0 | 8.4 | 93.2 | [82] |
| CePMo | 150–180 | 8 | 1 | 0.004 **** | 8.2 | 4.8 | 3.4 | 99.9 | [82] |
| FePMo | 150–180 | 8 | 1 | 0.004 **** | 22.3 | 9.9 | 11.6 | 96.4 | [82] |
| NiPMo | 150–180 | 8 | 1 | 0.004 **** | 19.5 | 9.5 | 9.0 | 94.9 | [82] |
| Cu _{1.5} PMo ₁₂ O ₄₀ /SiO ₂ | 150–180 | 8 | 1 | 0.2 | 25.2 | 13.5 | 11.5 | 99.2 | [83, 84] |
| HPMo/TiO ₂ | 160–180 | 8 | 1 | 0.04 | 44.7 | 22.8 | 21.7 | 99.6 | [85] |
| ZnPWO/TiO ₂ | N.A. *** | N.A. *** | N.A. *** | N.A. *** | 12.8 | N.A. *** | 10.7 | 83.6 | [85] |

* Transesterification selectivity includes both DPC and MPC. *** N.A. Not Available. **** N.D. Not Detected.

** Conversion is calculated based on phenol unless stated otherwise. ***** Calculated on mole basis.

Hu et al. [86] first employed transition-metal-substituted heteropolyacid salts (TMS-POM) $K_5[PW_{11}O_{39}M(H_2O)]/TiO_2$ ($M = Mn, Co, Ni, Cu, Zn$) as catalysts for transesterification. The results showed that the catalytic activity of transesterification was dependent on the type of transition metal in TMS-POM, with the Zn-substituted $K_5[PW_{11}O_{39}Zn(H_2O)]/TiO_2$ exhibiting the optimal activity. The conversion of phenol was 12.8%, with a selectivity of 83.6% for DPC. The authors proposed a mechanism where the substituted transition metal anchors the intermediate formed during transesterification. Initially, phenol acted on TMS-POM to remove water molecules, exposing the coordinating metal. Subsequently, coordination of the carbonyl oxygen of DMC with the transition metal polarized the carbonyl group, which was attacked by PhO^- after proton abstraction from phenol, resulting in the formation of intermediate (IV). Further transesterification or MPC disproportionation then yielded DPC.

Wang et al. [82] used various 12-phosphomolybdic acid salts as catalysts for transesterification. Zinc salts were found to exhibit the highest activity for transesterification. When the reaction temperature was 150–180 °C, PhOH/DMC = 1, and the reaction time was 12 h, the conversion of phenol reached 31%, with selectivities of 29% for MPC and 66.1% for DPC. Furthermore, they loaded heteropolyacid salts onto SiO₂ supports using an impregnation method [83,84] to prepare Cu_{1.5}PMo₁₂O₄₀/SiO₂ catalysts and investigated the effect of the catalyst calcination temperature. The results showed that calcination at 400 °C retained the Keggin structure of the heteropolyacid, while calcination above 450 °C led to the decomposition of the heteropolyacid salt, producing α -MoO₃. Cu²⁺ doping enhanced the stability of the Keggin structure, inhibiting the formation of the MoO₃ phase. The catalytic activity exhibited an increasing trend followed by a decrease with increasing calcination temperature, reaching a maximum at 400 °C, indicating the significant role of Keggin units in catalytic activity. For the catalyst calcined at 400 °C, the conversion of phenol was 25%, and the transesterification selectivity reached 99.5%.

In addition to using heteropolyacid salts, they also attempted to directly use heteropolyacids as catalysts [85]. By directly loading 12-phosphomolybdic acid onto TiO₂ surfaces using a one-step in situ synthesis method, they achieved highly dispersed phosphomolybdic acid on the TiO₂ support, stabilizing the Keggin structure of phosphomolybdic acid. Under the conditions of a TiO₂-to-phosphomolybdic acid weight ratio of 1:1, a calci-

nation temperature of 300 °C, and a reaction time of 10 h, the conversion of phenol and transesterification selectivity reached 50.4% and 99.4%, respectively. Stability experiments revealed catalyst deactivation, with the conversion of phenol decreasing from 44.7% to 29.5% after four consecutive runs, while the transesterification selectivity remained at 99%. The characterization of the deactivated catalysts revealed that the Mo⁶⁺ of phosphomolybdic acid was partially reduced to Mo⁵⁺ after the reaction, which may have been the cause of deactivation.

In addition to heteropolyacids and heteropolyacid salts, there are also reports of monopolyacid salts as catalysts. Kim et al. [87] reported the activity of a novel ammonium molybdate catalyst, (NH₄)₈Mo₁₀O₃₄, for transesterification, which was formed by the calcination of commercial ammonium molybdate ((NH₄)₆Mo₇O₂₄·4H₂O) at 150 °C. The homogeneously dissolved Mo species formed during the reaction played an important role, and the turnover frequency (TOF) of this Mo species was superior to that of the reported Pb species.

5. Bridge between Homogeneous and Heterogeneous Catalysis: Ionic Liquids

Ionic liquids are a type of catalytic material that has been increasingly used in recent years. Their high thermal stability and ease of separation make them exhibit characteristics of both homogeneous and heterogeneous catalysts. Ionic liquids possess the intrinsic Lewis acidity of cations and can therefore be used as catalysts for transesterification. The activity of ionic liquid catalysts is summarized in Table 14.

Table 14. Activity of ionic-liquid-based catalysts.

| Catalyst | Temperature (°C) | Time (h) | PhOH/DMC | Cat/PhOH (in Mass) | Conversion ** (%) | MPC Yield (%) | DPC Yield (%) | Transesterification Selectivity * (%) | Ref. |
|---|------------------|----------|-----------|--------------------|-------------------|---------------|---------------|---------------------------------------|------|
| Bu ₂ SnO–[NMP][HSO ₄] | 180–200 | 12 | 1 | 0.021 | 30.7 | 2.4 | 12.8 | 99.9 | [88] |
| Bu ₂ SnO–[HMim][pTSA] | 180–200 | 12 | 1 | 0.021 | 29.3 | 4.9 | 12.2 | 99.9 | [88] |
| Bu ₂ SnO–[C ₄ Mim][pTSA] | 180–200 | 12 | 1 | 0.021 | 35 | 9.4 | 12.8 | 99.9 | [88] |
| Bu ₂ SnO–[BMim]Cl[ZnCl ₂] | 180–200 | 12 | 1 | 0.021 | 38.5 | 2.8 | 17.8 | 99.5 | [88] |
| Bu ₂ SnO–[BMim]Cl[ZnCl ₂] ₂ | 180–200 | 12 | 1 | 0.021 | 31.4 | 12.1 | 9.4 | 97.7 | [88] |
| Bu ₂ SnO–[ChCl][ZnCl ₂] | 180–200 | 12 | 1 | 0.021 | 39 | 1.8 | 18.6 | 99.9 | [88] |
| Bu ₂ SnO–[ChCl][ZnCl ₂] ₂ | 180–200 | 12 | 1 | 0.021 | 29.3 | 7.5 | 10.7 | 99.9 | [88] |
| Bu ₂ SnO–[ChCl][SnCl ₂] | 180–200 | 12 | 1 | 0.021 | 18.1 | 3.1 | 7.5 | 99.9 | [88] |
| Bu ₂ SnO–[ChCl][SnCl ₂] ₂ | 180–200 | 12 | 1 | 0.021 | 14.5 | 1.5 | 6.4 | 97.5 | [88] |
| Bu ₂ SnO–[ChCl][FeCl ₃] ₂ | 180–200 | 12 | 1 | 0.021 | 14.9 | 4.3 | 5.3 | 99.9 | [88] |
| [SBA–15-IL–CH ₃]Br *** | 170 | 2 | N.A. | 0.035 | 51.0 | N.A. | 50.8 | 99.6 | [89] |
| [SBA–15-IL–OH]Br *** | 170 | 2 | N.A. | 0.035 | 80.5 | N.A. | 80.2 | 99.6 | [89] |
| [SBA–15-IL–COOH]Br *** | 170 | 2 | N.A. | 0.035 | 81.2 | N.A. | 73.4 | 90.4 | [89] |
| [SBA–15-IL–NH ₂]Br *** | 170 | 2 | N.A. **** | 0.035 | 82.6 | N.A. | 74.0 | 89.6 | [89] |
| [SBA–15-IL–SO ₄ H]Br *** | 170 | 2 | N.A. **** | 0.035 | 84.6 | N.A. | 74.4 | 87.9 | [89] |
| [SBA–15-IL–2C–OH]Br *** | 170 | 2 | N.A. **** | 0.035 | 80.1 | N.A. | 79.6 | 99.4 | [89] |
| [SBA–15-IL–4C–OH]Br *** | 170 | 2 | N.A. **** | 0.035 | 77.4 | N.A. | 76.8 | 99.2 | [89] |
| [SBA–15-IL–6C–OH]Br *** | 170 | 2 | N.A. **** | 0.035 | 75.7 | N.A. | 75.2 | 99.3 | [89] |
| [SBA–15-IL–8C–OH]Br *** | 170 | 2 | N.A. **** | 0.035 | 74.7 | N.A. | 74.3 | 99.5 | [89] |
| [SBA–15-IL–OH]BF ₄ *** | 170 | 2 | N.A. **** | 0.035 | 79.6 | N.A. | 71.8 | 90.2 | [89] |
| [SBA–15-IL–OH]PF ₆ *** | 170 | 2 | N.A. **** | 0.035 | 77.2 | N.A. | 70.5 | 91.3 | [89] |
| [SBA–15-IL–OH]HSO ₄ *** | 170 | 2 | N.A. **** | 0.035 | 83.1 | N.A. | 70.8 | 85.2 | [89] |
| [SBA–15-IL–OH]OH *** | 170 | 2 | N.A. **** | 0.035 | 81.7 | N.A. | 70.2 | 85.9 | [89] |
| Na ₄ [Ti(H ₂ O)TiMo ₁₁ O ₃₉] | 160 | 6 | 0.5 | 0.015 | 37.32 | 20.43 | 14.93 | 94.74 | [90] |
| Bmim ₆ [Sn(H ₂ O)TiMo ₁₁ O ₃₉] | 160 | 6 | 0.5 | 0.015 | 31.92 | 15.92 | 15.56 | 98.62 | [90] |
| Bmim ₆ [Zn(H ₂ O)TiMo ₁₁ O ₃₉] | 160 | 6 | 0.5 | 0.015 | 23.45 | 11.25 | 11.46 | 96.84 | [90] |
| Bmim ₆ [Fe(H ₂ O)TiMo ₁₁ O ₃₉] | 160 | 6 | 0.5 | 0.015 | 29.10 | 9.45 | 18.82 | 97.15 | [90] |
| Bmim ₆ [Cu(H ₂ O)TiMo ₁₁ O ₃₉] | 160 | 6 | 0.5 | 0.015 | 21.47 | 10.64 | 9.51 | 93.85 | [90] |
| Bmim ₄ [Ti(H ₂ O)TiMo ₁₁ O ₃₉] | 160 | 6 | 0.5 | 0.015 | 42.45 | 18.38 | 23.50 | 98.65 | [90] |
| Bmim ₄ [Pb(H ₂ O)TiMo ₁₁ O ₃₉] | 160 | 6 | 0.5 | 0.015 | 27.08 | 13.12 | 12.78 | 95.64 | [90] |

* Transesterification selectivity includes both DPC and MPC. ** Conversion is calculated based on phenol unless stated otherwise. *** MPC disproportionation. **** N.A. Not Available.

Ionic liquids were initially used as dopants in homogeneous catalysis. Bhanage et al. [88] discovered that using ionic liquids as dopants significantly increased the yield of DPC in transesterification catalyzed by dibutyltin oxide. They found that two types of ionic liquids, [NMP][HSO₄] and [ChCl][ZnCl₂], both exhibited good promoting effects, indicating that the Bronsted acidity or Lewis acidity of ionic liquids could promote transesterification.

Among them, dibutyltin oxide promoted by $[\text{ChCl}][\text{ZnCl}_2]$ achieved a phenol conversion of 31% and a transesterification selectivity of 99.9%.

Subsequently, ionic liquids were also attempted to be used as immobilized catalysts. Wang et al. [89] developed ionic liquids immobilized on SBA-15 mesoporous silica (the immobilization method and the prepared ionic liquids are shown in Figure 12) for MPC disproportionation. They screened ionic liquids with different functional groups and found that $[\text{SBA-15-IL-OH}]\text{Br}$ with an -OH group exhibited the best catalytic activity, with the conversion of toluene carbonate (MPC) reaching 80.5% and a DPC selectivity of 99.6%. This was attributed to the suitable catalytic performance of the hydroxyl group. Amino and carboxyl groups with strong acidity/alkalinity catalyzed decarboxylation side reactions to produce anisole, while methyl groups with weak acidity, although exhibiting good DPC selectivity, had lower conversions.

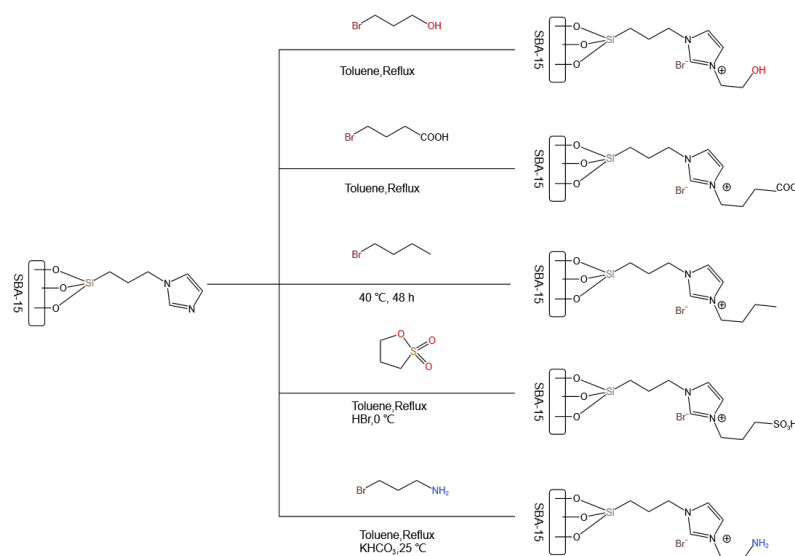


Figure 12. Strategy diagram of SBA-15 immobilizing ionic liquid (redrawn, data from [89]).

Guo et al. [90] developed polyoxometalate ionic liquids for transesterification, among which $\text{Bmim}_4[\text{Ti}(\text{H}_2\text{O})\text{TiMo}_{11}\text{O}_{39}]$ (Bmim = 1-butyl-3-methylimidazolium cation) exhibited the best catalytic performance. With a molar ratio of DMC to phenol of 2:1, a reaction temperature of 180 °C, a catalyst dosage accounting for 1.5% of the total mass of raw materials, and a reaction time of 8 h, the conversion of phenol reached 46.17%, and the total selectivity of the products MPC and DPC was 98.89%. Experimental processes indicated that when the temperature of the reaction system reached 100–120 °C, the polyoxometalate ionic liquid melted and became homogeneous with the reaction system. After the temperature decreased to room temperature, the polyoxometalate ionic liquid solidified and separated from the reaction system, serving as a temperature-controlled phase-transfer catalyst characterized as “homogeneous at high temperature and separated at low temperature”. However, the catalyst showed significant deactivation, with a noticeable decrease in performance after four to five cycles of use, necessitating the addition of fresh catalyst to maintain catalytic activity. Mechanistic experiments indicated that the catalytic active center was the Ti site in the polyoxometalate.

6. Potential Alternative Routes: Dimethyl Oxalate and Phenyl Acetate as Raw Materials

In addition to the process of transesterification between dimethyl carbonate and phenol esters to produce diphenyl carbonate (DPC), there are also processes involving the exchange of dimethyl oxalate (DMO) with phenol esters and DMC with phenyl acetate (PA) esters.

In the reaction between DMO and phenol, the intermediate methyl phenyl oxalate (MPO) is first generated, which further reacts with phenol to produce diphenyl oxalate

(DPO), or MPO undergoes a disproportionation reaction to generate DPO and DMO. The generated DPO further undergoes decarbonylation to produce DPC. Thermodynamic analysis shows that the reaction equilibrium constant between DMO and phenol is very small, requiring the continuous separation of the product methanol from the reaction system. However, because no azeotrope is formed in this reaction system and there is a large difference in boiling points, the separation of methanol is relatively easy, reducing the design difficulty of the reactor and facilitating industrialization. However, the decarbonylation reaction of the intermediate DPO increases the complexity of the entire process. Meanwhile, phenol can undergo methylation with DMO to produce the byproduct anisole, and controlling the side reaction is beneficial to improving the selectivity and yield of DPC. Lewis acid catalysts such as organotitanium and organotin compounds are generally used as catalysts in this reaction system. There are also many reports on heterogeneous catalysts, such as tin-modified titanium silicalite [91–93] and supported metal oxides (such as MoO_3) [94–99]. Compared with homogeneous catalysts, heterogeneous catalysts are easy to separate and recycle, but there is still much room for improvement in terms of activity and stability. Future research will focus on improving the activity and stability of heterogeneous catalysts to meet industrial requirements.

In the reaction between DMC and PA, the intermediate methyl phenyl carbonate (MPC) is first generated, which further reacts with PA to produce DPC and methyl acetate (MA), or MPC undergoes disproportionation to generate DPC and DMC. Given the significant limitations imposed by the thermodynamics of DMO with phenol and DMC with phenol, thermodynamic calculations show that the equilibrium constant of the reaction of DMC with PA is 10^5 times that of the reaction of DMC with phenol under the same conditions, which is more favorable thermodynamically. However, the reaction is still constrained by thermodynamics. Meanwhile, the equilibrium constants for the transesterification and disproportionation reactions of DMC with PA are close, so this route does not use the two-step method used in the reaction between DMC and phenol to make the process more thermodynamically favorable. Instead, a one-step method is mainly adopted to simplify the reaction process and reduce equipment investment. In this reaction system, no azeotrope is formed, and the main byproduct of the reaction is MA. MA can be cracked to produce methyl vinyl ketone and methanol under certain conditions. Methyl vinyl ketone can react with phenol to generate PA, and methanol can be used to generate DMC. Theoretically, MA can be fully utilized. Through a reasonable process design, a 100% atom utilization rate can be achieved. The catalysts for the reaction between DMC and PA mainly include Lewis acid catalysts and homogeneous catalysts such as titanium alkoxides [100], as well as heterogeneous catalysts such as supported molybdenum oxide and molybdenum–titanium composite oxides [101–106]. However, the performance of the catalysts still needs to be improved. The reaction between DMC and PA is a green synthesis process for DPC production with great development value and application prospects. Further research is needed on reactor design, process route optimization, and efficient catalyst development to accelerate industrialization.

7. Conclusions and Prospects

Transesterification for the production of dimethyl carbonate is a green, environmentally friendly, and non-polluting process, which is replacing the phosgene method as the mainstream process for diphenyl carbonate production. The development of catalysts is mainly based on catalytic reaction processes divided into homogeneous and heterogeneous catalysts. To date, only homogeneous catalysts have been industrialized, but both homogeneous and heterogeneous catalysts still have significant research value:

1. Homogeneous catalysts, represented by Ti-based, Sn-based, and Pb-based catalysts, follow the Lewis acid catalysis mechanism. The catalytic centers rely on the Lewis acidity of the metal center: Lewis acid sites first activate the carbonyl group of DMC, followed by the nucleophilic addition of phenol, ultimately generating DPC. Currently, Pb-based catalysts are no longer used due to environmental issues, and

- Ti-based catalysts are the mainstream. However, Ti-based catalysts, mainly titanium alkoxides, are still limited by their poor stability.
2. Heterogeneous catalysts include oxides, molecular sieves, hydrotalcites, and polyoxometalates/polyoxometalate salts, among others. Their design concept borrows from the catalysis of metal Lewis acid centers, with the basic idea being the heterogenization of homogeneous catalysts. Among them, TiO₂-based catalysts are more frequently reported, but their activity and stability still need to be improved.
 3. New types of catalysts, represented by ionic liquids, combining the characteristics of homogeneous and heterogeneous catalysts, can act as homogeneous catalysts during the reaction and be separated from the catalytic system after the reaction, which is the direction of future basic research on catalysts. However, they are still limited by high preparation costs, complex preparation processes, and issues related to the loss of catalytically active components. Additionally, their catalytic reaction mechanism still needs to be further clarified.
 4. Currently, the transesterification reaction between dimethyl carbonate and phenol is still limited by thermodynamics, with a relatively small equilibrium constant. However, using dimethyl oxalate or phenyl acetate for transesterification can, to some extent, increase the equilibrium constant of the transesterification and alleviate the thermodynamic constraints.

Funding: This research received no external funding.

Data Availability Statement: Data are available on request from the authors.

Conflicts of Interest: The authors declare no conflicts of interest.

Abbreviations

The following abbreviations are used in this manuscript:

| | |
|------|-------------------------|
| DMC | Dimethyl carbonate |
| DPC | Diphenyl carbonate |
| MPC | Methyl phenyl carbonate |
| PhOH | Phenol |
| DMO | Dimethyl oxalate |
| PA | Phenyl acetate |
| DPO | Diphenyl oxalate |

References

1. Freitag, D.; Fengler, G.; Morbitzer, L. Routes to new aromatic polycarbonates with special material properties. *Angew. Chem. Int. Ed. Engl.* **1991**, *30*, 1598–1610. [[CrossRef](#)]
2. Domingo-Espin, M.; Puigoriol-Forcada, J.M.; Garcia-Granada, A.A.; Llumà, J.; Borros, S.; Reyes, G. Mechanical property characterization and simulation of fused deposition modeling Polycarbonate parts. *Mater. Des.* **2015**, *83*, 670–677. [[CrossRef](#)]
3. Park, S.J.; Lee, J.E.; Lee, H.B.; Park, J.; Lee, N.K.; Son, Y.; Park, S.H. 3D printing of bio-based polycarbonate and its potential applications in ecofriendly indoor manufacturing. *Addit. Manuf.* **2020**, *31*, 100974. [[CrossRef](#)]
4. Sai, T.; Ran, S.; Guo, Z.; Yan, H.; Zhang, Y.; Wang, H.; Song, P.; Fang, Z. Transparent, highly thermostable and flame retardant polycarbonate enabled by rod-like phosphorous-containing metal complex aggregates. *Chem. Eng. J.* **2021**, *409*, 128223. [[CrossRef](#)]
5. Yu, W.; Maynard, E.; Chiaradia, V.; Arno, M.C.; Dove, A.P. Aliphatic polycarbonates from cyclic carbonate monomers and their application as biomaterials. *Chem. Rev.* **2021**, *121*, 10865–10907. [[CrossRef](#)] [[PubMed](#)]
6. Mu, X.; Jin, Z.; Chu, F.; Cai, W.; Zhu, Y.; Yu, B.; Song, L.; Hu, Y. High-performance flame-retardant polycarbonate composites: Mechanisms investigation and fire-safety evaluation systems establishment. *Compos. Part Eng.* **2022**, *238*, 109873. [[CrossRef](#)]
7. Bian, Y.; Liu, Q.; Feng, Z.; Hua, J.; Xie, H.; Chen, S.; Cai, Y.; Yao, X.; Luo, S. High-speed penetration dynamics of polycarbonate. *Int. J. Mech. Sci.* **2022**, *223*, 107250. [[CrossRef](#)]
8. Fromel, M.; Pester, C.W. Polycarbonate Surface Modification via Aqueous SI-PET-RAFT. *Macromolecules* **2022**, *55*, 4907–4915. [[CrossRef](#)]
9. Mehrara, R.; Malekie, S.; Kotahi, S.M.S.; Kashian, S. Introducing a novel low energy gamma ray shield utilizing polycarbonate bismuth oxide composite. *Sci. Rep.* **2021**, *11*, 10614. [[CrossRef](#)] [[PubMed](#)]
10. Kim, W.B.; Joshi, U.A.; Lee, J.S. Making polycarbonates without employing phosgene: An overview on catalytic chemistry of intermediate and precursor syntheses for polycarbonate. *Ind. Eng. Chem. Res.* **2004**, *43*, 1897–1914. [[CrossRef](#)]

11. Darensbourg, D.J. Making plastics from carbon dioxide: Salen metal complexes as catalysts for the production of polycarbonates from epoxides and CO₂. *Chem. Rev.* **2007**, *107*, 2388–2410. [[CrossRef](#)] [[PubMed](#)]
12. Huang, J.; Worch, J.C.; Dove, A.P.; Coulembier, O. Update and challenges in carbon dioxide-based polycarbonate synthesis. *ChemSusChem* **2020**, *13*, 469–487. [[CrossRef](#)] [[PubMed](#)]
13. Gong, J.; Ma, X.; Wang, S. Phosgene-free approaches to catalytic synthesis of diphenyl carbonate and its intermediates. *Appl. Catal. Gen.* **2007**, *316*, 1–21. [[CrossRef](#)]
14. Song, Z.; Jin, W.; Gao, F.; Jin, X. Recent advances in catalyst development for transesterification of dialkyl carbonates with phenol. *Ind. Eng. Chem. Res.* **2020**, *59*, 20630–20645. [[CrossRef](#)]
15. Lee, H.Y.; Novita, F.J.; Weng, K.C. Hybrid heat-integrated design and control for a diphenyl carbonate reactive distillation process. *Chem. Eng. Process.-Process. Intensif.* **2021**, *162*, 108344. [[CrossRef](#)]
16. Otera, J. Transesterification. *Chem. Rev.* **1993**, *93*, 1449–1470. [[CrossRef](#)]
17. Shen, W.; Ge, Q.; Gu, K.; Nie, Y.; Jiao, L.; Zhu, Z.; Fang, Y. Stable organic titanium catalysts and reactive distillation used for the transesterification of dimethyl carbonate with phenol. *Chem. Eng. Technol.* **2020**, *43*, 2359–2364. [[CrossRef](#)]
18. Yin, X.; Zeng, Y.; Yao, J.; Zhang, H.; Deng, Z.; Wang, G. Kinetic modeling of the transesterification reaction of dimethyl carbonate and phenol in the reactive distillation reactor. *Ind. Eng. Chem. Res.* **2014**, *53*, 19087–19093. [[CrossRef](#)]
19. Aihua, X.; Mingqing, Z.; Zhimin, H.; Jianping, Z. Thermodynamic analysis of synthesis of diphenyl carbonate by transesterification of dimethyl carbonate and phenol. *Chem. Eng.* **2006**, *34*, 40–43.
20. Mei, F.; Li, G. The thermodynamic properties and homogeneous catalysts for the synthesis of diphenyl carbonate by transesterification of dimethyl carbonate with phenol. *Chin. J. Synth. Chem.* **2003**, *11*, 320–326.
21. Guo, X.; Shi, Y.; Zheng, H.; Cheng, J.; Zhao, X.; Yang, B. Thermodynamic study on diphenyl carbonate synthesis with different feedstocks. *J. Chem. Eng. Chin. Univ.* **2016**, *30*, 754–760.
22. Haubrock, J.; Raspe, M.; Versteeg, G.F.; Kooijman, H.A.; Taylor, R.; Hogendoorn, J.A. Reaction from dimethyl carbonate to diphenyl carbonate. 1. experimental determination of the chemical equilibria. *Ind. Eng. Chem. Res.* **2008**, *47*, 9854–9861. [[CrossRef](#)]
23. Sun, W.; Shao, J.; Xi, Z.; Zhao, L. Thermodynamics and kinetics of transesterification reactions to produce diphenyl carbonate from dimethyl carbonate catalyzed by tetrabutyl titanate and dibutyltin oxide. *Can. J. Chem. Eng.* **2017**, *95*, 353–358. [[CrossRef](#)]
24. Bandsode, S.P.; Besta, C.S. Dynamic analysis and decentralised control system design for diphenyl carbonate reactive distillation process. *Indian Chem. Eng.* **2020**, *64*, 151–161. [[CrossRef](#)]
25. Mofijur, M.; Siddiki, S.Y.A.; Shuvho, M.B.A.; Djavanroodi, F.; Fattah, I.R.; Ong, H.C.; Chowdhury, M.; Mahlia, T. Effect of nanocatalysts on the transesterification reaction of first, second and third generation biodiesel sources—A mini-review. *Chemosphere* **2021**, *270*, 128642. [[CrossRef](#)] [[PubMed](#)]
26. Orege, J.I.; Oderinde, O.; Kifle, G.A.; Ibikunle, A.A.; Raheem, S.A.; Ejeromedoghene, O.; Okeke, E.S.; Olukowi, O.M.; Orege, O.B.; Fagbohun, E.O.; et al. Recent advances in heterogeneous catalysis for green biodiesel production by transesterification. *Energy Convers. Manag.* **2022**, *258*, 115406. [[CrossRef](#)]
27. Nayab, R.; Imran, M.; Ramzan, M.; Tariq, M.; Taj, M.B.; Akhtar, M.N.; Iqbal, H.M. Sustainable biodiesel production via catalytic and non-catalytic transesterification of feedstock materials—A review. *Fuel* **2022**, *328*, 125254. [[CrossRef](#)]
28. Maleki, B.; Ashraf Talesh, S.; Mansouri, M. Comparison of catalysts types performance in the generation of sustainable biodiesel via transesterification of various oil sources: A review study. *Mater. Today Sustain.* **2022**, *18*, 100157. [[CrossRef](#)]
29. Gao, J.; Yao, J.; Mei, H.; Wang, G. Transesterification of dimethyl carbonate and phenol with titanate catalysts. *Chin. J. Catal.* **2001**, *22*, 406–407.
30. Niu, H.; Yao, J.; Wang, Y.; Wang, G. Cp₂TiCl₂ used as a catalyst for the transesterification between dimethyl carbonate and phenol to diphenyl carbonate. *J. Mol. Catal. Chem.* **2005**, *235*, 240–243. [[CrossRef](#)]
31. Hongying, N.; Haiming, G.; Jie, Y.; Yue, W.; Gongying, W. Transesterification of dimethyl carbonate and phenol to diphenyl carbonate catalyzed by titanocene complexes. *Acta Chim. Sin.* **2006**, *64*, 1269.
32. Rongzhi, T.; Songlin, W.; Yuanzhuo, Z.; Tong, C.; Gongying, W. Catalytic property of titanyl acetate in the transesterification reaction of dimethyl carbonate and phenol. *Chem. J. Chin. Univ.* **2014**, *35*, 2418–2424.
33. Wang, S.; Chen, T.; Wang, G.; Cui, C.; Niu, H.; Li, C. Influence of coordination groups on the catalytic performances of organo-titanium compounds for disproportionation of methyl phenyl carbonate to synthesize diphenyl carbonate. *Appl. Catal. Gen.* **2017**, *540*, 1–6. [[CrossRef](#)]
34. Lee, H.; Joon Kim, S.; Sung Ahn, B.; Koo Lee, W.; Sik Kim, H. Role of sulfonic acids in the Sn-catalyzed transesterification of dimethyl carbonate with phenol. *Catal. Today* **2003**, *87*, 139–144. [[CrossRef](#)]
35. Du, Z.; Chen, S.; Shen, C.; Zhou, B.; Huang, L.; Wang, G.; Wu, Y. Effect of copper compounds on the synthesis of diphenyl carbonate from transesterification catalyzed by n-Bu₂SnO. *Adv. Mater. Res.* **2012**, *396–398*, 759–763.
36. Du, Z.; Kang, W.; Cheng, T.; Yao, J.; Wang, G. Novel catalytic systems containing n-BuSn(O)OH for the transesterification of dimethyl carbonate and phenol. *J. Mol. Catal. Chem.* **2006**, *246*, 200–205. [[CrossRef](#)]
37. Shaikh, A.A.G.; Sivaram, S. Dialkyl and diaryl carbonates by carbonate interchange reaction with dimethyl carbonate. *Ind. Eng. Chem. Res.* **1992**, *31*, 1167–1170. [[CrossRef](#)]
38. Jie, Y.; Junjie, G.; Yi, Z.; Yue, W.; Gongying, W. Influences of catalysts on the transesterification of dimethyl carbonate and phenol. *Chin. J. Appl. Chem.* **2003**, *20*, 898–902.

39. Yue, W.; Jie, Y.; Yi, Z.; Gongying, W. Mechanism study of di-n-butyltin oxide catalyzed transesterification of dimethyl carbonate with phenol. *Acta Chim. Sin.* **2005**, *63*, 603.
40. Lee, H.; Yong Bae, J.; Kwon, O.S.; Joon Kim, S.; Deuk Lee, S.; Sik Kim, H. Sulfonate-bonded tin complexes for the production of diphenyl carbonate. *J. Organomet. Chem.* **2004**, *689*, 1816–1820. [[CrossRef](#)]
41. Fukuoka, S.; Fukawa, I.; Tojo, M.; Oonishi, K.; Hachiya, H.; Aminaka, M.; Hasegawa, K.; Komiya, K. A novel non-phosgene process for polycarbonate production from CO₂: Green and sustainable chemistry in practice. *Catal. Surv. Asia* **2010**, *14*, 146–163. [[CrossRef](#)]
42. Fuming, M.; Guangxing, L.; Jin, N.; Huibi, X. A novel catalyst for transesterification of dimethyl carbonate with phenol to diphenyl carbonate: Samarium trifluoromethanesulfonate. *J. Mol. Catal. Chem.* **2002**, *184*, 465–468. [[CrossRef](#)]
43. Niu, H.; Guo, H.; Yao, J.; Wang, Y.; Wang, G. Transesterification of dimethyl carbonate and phenol to diphenyl carbonate catalyzed by samarium diiodide. *J. Mol. Catal. Chem.* **2006**, *259*, 292–295. [[CrossRef](#)]
44. Gao, Y.; Li, Z.; Su, K.; Cheng, B. Excellent performance of TiO₂ (B) nanotubes in selective transesterification of DMC with phenol derivatives. *Chem. Eng. J.* **2016**, *301*, 12–18. [[CrossRef](#)]
45. Kim, W.B.; Lee, J.S. Gas phase transesterification of dimethyl carbonate and phenol over supported titanium dioxide. *J. Catal.* **1999**, *185*, 307–313. [[CrossRef](#)]
46. Qu, Y.; Wang, S.; Chen, T.; Wang, G. Zn-promoted synthesis of diphenyl carbonate via transesterification over Ti–Zn double oxide catalyst. *Res. Chem. Intermed.* **2017**, *43*, 2725–2735. [[CrossRef](#)]
47. Xin, G.; Bijing, L.; Jing, H.; Tong, C.; Gongying, W.; Xuteng, H. Effect of the surfactant on the catalytic activity of TiO₂/CNT for transesterification between dimethyl carbonate and phenol. *Acta Chim. Sin.* **2011**, *69*, 2328.
48. Qu, Y.; Yang, H.; Wang, S.; Chen, T.; Wang, G. High selectivity to diphenyl carbonate synthesized via transesterification between dimethyl carbonate and phenol with C60-doped TiO₂. *Chem. Res. Chin. Univ.* **2017**, *33*, 804–810. [[CrossRef](#)]
49. Yang, H.; Xiao, Z.; Qu, Y.; Chen, T.; Chen, Y.; Wang, G. The role of RGO in TiO₂–RGO composites for the transesterification of dimethyl carbonate with phenol to diphenyl carbonate. *Res. Chem. Intermed.* **2018**, *44*, 799–812. [[CrossRef](#)]
50. Tang, R.; Chen, T.; Chen, Y.; Zhang, Y.; Wang, G. Core-shell TiO₂@SiO₂ catalyst for transesterification of dimethyl carbonate and phenol to diphenyl carbonate. *Chin. J. Catal.* **2014**, *35*, 457–461. [[CrossRef](#)]
51. Kim, W.B.; Lee, J.S. A new process for the synthesis of diphenyl carbonate from dimethyl carbonate and phenol over heterogeneous catalysts. *Catal. Lett.* **1999**, *59*, 83–88. [[CrossRef](#)]
52. Weiqing, Z.; Xinqiang, Z.; Wang, Y.; Zhang, J. Synthesis of diphenyl carbonate by transesterification over lead and zinc double oxide catalyst. *Appl. Catal. Gen.* **2004**, *260*, 19–24. [[CrossRef](#)]
53. Cao, M.; Meng, Y.; Lu, Y. Synthesis of diphenyl carbonate from dimethyl carbonate and phenol using O₂-promoted PbO/MgO catalysts. *Catal. Commun.* **2005**, *6*, 802–807. [[CrossRef](#)]
54. Wang, S.; Li, C.; Xiao, Z.; Chen, T.; Wang, G. Highly efficient and stable PbO–ZrO₂ catalyst for the disproportionation of methyl phenyl carbonate to synthesize diphenyl carbonate. *J. Mol. Catal. Chem.* **2016**, *420*, 26–33. [[CrossRef](#)]
55. Wang, S.; Jiang, N.; Liang, L.; Niu, H.; Chen, T.; Wang, G. A facile route to prepare PbZr nanocomposite catalysts for the efficient synthesis of diphenyl carbonate. *Catal. Lett.* **2021**, *151*, 3250–3260. [[CrossRef](#)]
56. Hao, Y.; Wangming, H.; Lvming, S. Transesterification of dimethyl carbonate and phenol over PbO–Yb₂O₃ catalyst. *J. Chem. Eng. Chin. Univ.* **2007**, *21*, 146–149.
57. Wang, S.; Niu, H.; Wang, J.; Chen, T.; Wang, G.; Zhang, J. Highly effective transformation of methyl phenyl carbonate to diphenyl carbonate with recyclable Pb nanocatalyst. *RSC Adv.* **2019**, *9*, 20415–20423. [[CrossRef](#)] [[PubMed](#)]
58. Li, Z.; Yang, G.; Li, Y.; Zheng, H.; Cui, L. PbTiO₃ catalyst for transesterification of dimethyl carbonate with phenol. *J. Taiyuan Univ. Technol.* **2010**, *41*, 723–727.
59. Li, Z.; Wang, Y.; Ding, X.; Zhao, X. Investigation on the deactivation cause of lead-zinc double oxide for the synthesis of diphenyl carbonate by transesterification. *J. Nat. Gas Chem.* **2009**, *18*, 104–109. [[CrossRef](#)]
60. Wang, S.; Niu, H.; Guo, M.; Wang, J.; Chen, T.; Wang, G. Effect of zirconia polymorph on the synthesis of diphenyl carbonate over supported lead catalysts. *Mol. Catal.* **2019**, *468*, 117–124. [[CrossRef](#)]
61. Fu, Z.H.; Ono, Y. Two-step synthesis of diphenyl carbonate from dimethyl carbonate and phenol using MoO₃/SiO₂ catalysts. *J. Mol. Catal. Chem.* **1997**, *118*, 293–299. [[CrossRef](#)]
62. Tong, D.; Chen, T.; Ma, F.; Kang, T.; Lei, Y.; Hu, J.; Wang, Y.; Wang, G. Transesterification of dimethyl carbonate with phenol over a bimetallic molybdenum and copper catalyst. *React. Kinet. Catal. Lett.* **2008**, *94*, 121–129. [[CrossRef](#)]
63. Wang, S.; Zhang, Y.; Chen, T.; Wang, G. Preparation and catalytic property of MoO₃/SiO₂ for disproportionation of methyl phenyl carbonate to diphenyl carbonate. *J. Mol. Catal. Chem.* **2015**, *398*, 248–254. [[CrossRef](#)]
64. Li, Y.; He, S. Enhanced catalytic behavior for synthesis of diphenyl carbonate over SBA-16 composited with α-MoO₃. *Mol. Cryst. Liq. Cryst.* **2022**, *757*, 125–137. [[CrossRef](#)]
65. Wang, C.; Guo, T.; Sun, M.; Li, C.; Guo, M.; Li, C.; Wang, Q. Transesterification of dimethyl carbonate with phenol to diphenyl carbonate over magnesium oxide nanosheets. *Sci. Adv. Mater.* **2018**, *10*, 779–784. [[CrossRef](#)]
66. Wang, Q.; Li, C.; Guo, M.; Luo, S.; Hu, C. Transesterification of dimethyl carbonate with phenol to diphenyl carbonate over hexagonal Mg(OH)₂ nanoflakes. *Inorg. Chem. Front.* **2015**, *2*, 47–54. [[CrossRef](#)]
67. Tong, D.S.; Yao, J.; Wang, Y.; Niu, H.Y.; Wang, G.Y. Transesterification of dimethyl carbonate with phenol to diphenyl carbonate over V₂O₅ catalyst. *J. Mol. Catal. Chem.* **2007**, *268*, 120–126. [[CrossRef](#)]

68. Tong, D.; Chen, T.; Yao, J.; Wang, Y.; Wang, G.; Shi, D.; Li, Z.; Chen, Z. V-Cu composite oxide catalyst for transesterification of dimethyl carbonate with phenol to diphenyl carbonate. *Chin. J. Catal.* **2007**, *28*, 190–192. [[CrossRef](#)]
69. Wang, Q.; Sun, M.M.; Guo, M.; Luo, S.J.; Li, C.H.; Hu, C.W. Heterogeneous transesterification of dimethyl carbonate and phenol to diphenyl carbonate over vanadium pentoxide microstructures. *Integr. Ferroelectr.* **2015**, *164*, 154–164. [[CrossRef](#)]
70. Li, Z.; Qin, Z.; Wang, J. Catalytic synthesis of diphenyl carbonate by transesterification of methyl-carbonate with phenol. *Petrochem. Technol.* **2006**, *35*, 528–532.
71. Wu, Q.; Xu, C.; Zhu, L.; Meng, X.; Xiao, F.S. Recent strategies for synthesis of metallosilicate zeolites. *Catal. Today* **2022**, *390–391*, 2–11. [[CrossRef](#)]
72. Deng, X.; Yang, D.; Li, W.; Chai, Y.; Wu, G.; Li, L. Chemistry of coordinatively unsaturated centers in zeolites. *Trends Chem.* **2023**, *5*, 892–905. [[CrossRef](#)]
73. Zhao, P.; Li, Z.; Zhang, Y.; Cui, D.; Guo, Q.; Dong, Z.; Qi, G.; Xu, J.; Deng, F. Tuning Lewis acid sites in TS-1 zeolites for hydroxylation of anisole with hydrogen peroxide. *Microporous Mesoporous Mater.* **2022**, *335*, 111840. [[CrossRef](#)]
74. Ravi, M.; Sushkevich, V.L.; van Bokhoven, J.A. Towards a better understanding of Lewis acidic aluminium in zeolites. *Nat. Mater.* **2020**, *19*, 1047–1056. [[CrossRef](#)] [[PubMed](#)]
75. Shudong, Z.; Chenghua, X.; Liangrong, F.; Fali, Q. Synthesis of diphenyl carbonate over Ti- β molecular sieves. *Fine Chem.* **2005**, *22*, 115–117.
76. Luo, S.; Chen, T.; Tong, D.; Zeng, Y.; Lei, Y.; Wang, G. Synthesis of diphenyl carbonate via transesterification catalyzed by HMS mesoporous molecular sieves containing heteroelements. *Chin. J. Catal.* **2007**, *28*, 937–939. [[CrossRef](#)]
77. Zhang, J.; Gao, Y.; Zhang, J.; Zhao, J.; Shen, H. Synthesis and characterization of TiO₂-V₂O₅-MCM-41 for catalyzing transesterification of dimethyl carbonate with phenol. *Chem. Cent. J.* **2018**, *12*. [[CrossRef](#)]
78. Yuanzhuo, Z.; Songlin, W.; Zhongliang, X.; Tong, C.; Gongying, W. Effect of silanol content in silica support on catalytic performance of silica-anchored organotin catalyst for transesterification. *CIESC J.* **2017**, *68*, 1892–1898.
79. Fuming, M.; Zhi, P.; Guangxing, L. The transesterification of dimethyl carbonate with phenol over Mg-Al-hydrotalcite catalyst. *Org. Process. Res. Dev.* **2004**, *8*, 372–375. [[CrossRef](#)]
80. Qinqin, Y.; Shu, W.; Rongxian, B.; Fuming, M.; Guangxing, L. Transesterification of dimethyl carbonate and phenol catalyzed by Zn-Al hydrotalcite. *Chem. J. Chin. Univ.* **2005**, *26*, 1502–1506.
81. Shu, W.; Qinqin, Y.; Jinming, H.; Rongxian, B.; Guangxing, L. Study on the catalytic activity, life time and deactivation of hydrotalcite-like catalysts in transesterification. *Acta Chim. Sin.* **2005**, *63*, 1575.
82. Chen, T.; Han, H.; Yao, J.; Wang, G. The transesterification of dimethyl carbonate and phenol catalyzed by 12-molybdophosphoric salts. *Catal. Commun.* **2007**, *8*, 1361–1365. [[CrossRef](#)]
83. Huajun, H.; Tong, C.; Jie, Y.; Gongying, W.; Desheng, Z.; Dachuan, S.; Zhiming, C. Effect of calcining temperature on structure and catalytic performance of SiO₂ supported Cu_{3/2}PMo₁₂O₄₀. *J. Mol. Catal.* **2006**, *20*, 496–499.
84. Han, H.; Chen, T.; Yao, J.; Wang, G. A heterogeneous catalyst for the transesterification of dimethyl carbonate and phenol to form diphenyl carbonate. *Chin. J. Catal.* **2006**, *27*, 7–8. [[CrossRef](#)]
85. Wang, S.; Tang, R.; Zhang, Y.; Chen, T.; Wang, G. 12-Molybdophosphoric acid supported on titania: A highly active and selective heterogeneous catalyst for the transesterification of dimethyl carbonate and phenol. *Chem. Eng. Sci.* **2015**, *138*, 93–98. [[CrossRef](#)]
86. Luo, S.; Chi, Y.; Sun, L.; Wang, Q.; Hu, C. Single-step catalytic synthesis of diphenyl carbonate over transition-metal-substituted Keggin-type tungstophosphoric acid. *Catal. Commun.* **2008**, *9*, 2560–2564. [[CrossRef](#)]
87. Tae Kim, Y.; Duck Park, E. Transesterification between dimethyl carbonate and phenol in the presence of (NH₄)₈Mo₁₀O₃₄ as a catalyst precursor. *Appl. Catal. Gen.* **2009**, *361*, 26–31. [[CrossRef](#)]
88. Deshmukh, K.M.; Qureshi, Z.S.; Dhake, K.P.; Bhanage, B.M. Transesterification of dimethyl carbonate with phenol using Brønsted and Lewis acidic ionic liquids. *Catal. Commun.* **2010**, *12*, 207–211. [[CrossRef](#)]
89. Wang, S.; Zhang, Q.; Cui, C.; Niu, H.; Wu, C.; Wang, J. Ionic liquids-SBA-15 hybrid catalysts for highly efficient and solvent-free synthesis of diphenyl carbonate. *Green Energy Environ.* **2023**, *8*, 183–193. [[CrossRef](#)]
90. Jiang, Z.; Wang, H.; Shan, L.; Zheng, R.; Zhao, X.; Liao, Z.; Guo, L. Preparation of temperature-controlled heteropolyacid ionic liquids and their application for synthesis of diphenyl carbonate. *Catal. Lett.* **2022**, *153*, 1308–1318. [[CrossRef](#)]
91. Ma, X.; Guo, H.; Wang, S.; Sun, Y. Transesterification of dimethyl oxalate with phenol over TS-1 catalyst. *Fuel Process. Technol.* **2003**, *83*, 275–286. [[CrossRef](#)]
92. Wang, S.; Ma, X.; Gong, J.; Gao, N.; Guo, H.; Yang, X.; Xu, G. Characterization and activity of stannum modified H β catalysts for transesterification of dimethyl oxalate with phenol. *Catal. Today* **2004**, *93–95*, 377–381. [[CrossRef](#)]
93. Ma, X.; Gong, J.; Wang, S.; He, F.; Guo, H.; Yang, X.; Xu, G. Characterization and reactivity of stannum modified titanium silicalite TS-1 catalysts for transesterification of dimethyl oxalate with phenol. *J. Mol. Catal. Chem.* **2005**, *237*, 1–8. [[CrossRef](#)]
94. Wang, S.; Ma, X.; Guo, H.; Gong, J.; Yang, X.; Xu, G. Characterization and catalytic activity of TiO₂/SiO₂ for transesterification of dimethyl oxalate with phenol. *J. Mol. Catal. Chem.* **2004**, *214*, 273–279. [[CrossRef](#)]
95. GONG, J.; MA, X.; WANG, S.; LIU, M.; YANG, X.; XU, G. Transesterification of dimethyl oxalate with phenol over MoO₃/SiO₂ catalysts. *J. Mol. Catal. Chem.* **2004**, *207*, 215–220. [[CrossRef](#)]
96. Wang, S.; Ma, X.; Gong, J.; Yang, X.; Guo, H.; Xu, G. Transesterification of dimethyl oxalate with phenol under SnO₂/SiO₂ catalysts. *Ind. Eng. Chem. Res.* **2004**, *43*, 4027–4030. [[CrossRef](#)]

97. Biradar, A.; Umbarkar, S.; Dongare, M. Transesterification of diethyl oxalate with phenol using MoO₃/SiO₂ catalyst. *Appl. Catal. Gen.* **2005**, *285*, 190–195. [[CrossRef](#)]
98. Liu, Y.; Ma, X.; Wang, S.; Gong, J. The nature of surface acidity and reactivity of MoO₃/SiO₂ and MoO₃/TiO₂-SiO₂ for transesterification of dimethyl oxalate with phenol: A comparative investigation. *Appl. Catal. Environ.* **2007**, *77*, 125–134. [[CrossRef](#)]
99. Yang, X.; Ma, X.; Wang, S.; Gong, J. Transesterification of dimethyl oxalate with phenol over TiO₂/SiO₂: Catalyst screening and reaction optimization. *AIChE J.* **2008**, *54*, 3260–3272. [[CrossRef](#)]
100. Cao, P.; Yang, J.; Yang, X.; Yao, J.; Wang, Y.; Wang, G. Organotitanium compound catalysts for transesterification of dimethyl carbonate and phenyl acetate to diphenyl carbonate. *Chin. J. Catal.* **2009**, *30*, 65–68. [[CrossRef](#)]
101. Cao, P.; Yang, X.; Tang, C.; Yang, J.; Yao, J.; Wang, Y.; Wang, G. Molybdenum trioxide catalyst for transesterification of dimethyl carbonate and phenyl acetate to diphenyl carbonate. *Chin. J. Catal.* **2009**, *30*, 853–855. [[CrossRef](#)]
102. Cao, P.; Yang, X.; Ma, F.; Tang, C.; Kang, T.; Wang, G. MoO₃ catalyst for transesterification of dimethyl carbonate and phenyl acetate to diphenyl carbonate. *Petrochem. Technol.* **2011**, *40*, 1037–1041.
103. Wang, L.; Yang, X.; Liu, L.; Wang, G. Transesterification of dimethyl carbonate and phenyl acetate to diphenyl carbonate over TiO₂/SiO₂ catalysts. *Petrochem. Technol.* **2012**, *41*, 770–777.
104. Tang, R.; Wang, S.; Zhang, Y.; Chen, T.; Wang, G. Catalytic property of titanyl acetate in the transesterification reaction of dimethyl carbonate and phenol. *Chem. J. Chin. Univ.* **2014**, *35*, 2418–2424.
105. Cao, P.; Wang, G. Supported MoO₃/SiO₂ catalyst for transesterification of dimethyl carbonate and phenyl acetate to diphenyl carbonate. *Acta Pet. Sin. (Petroleum Process. Sect.)* **2014**, *30*, 823–828.
106. Jia, B.; Cao, P.; Zhang, H.; Wang, G. Mesoporous amorphous TiO₂ shell-coated ZIF-8 as an efficient and recyclable catalyst for transesterification to synthesize diphenyl carbonate. *J. Mater. Sci.* **2019**, *54*, 9466–9477. [[CrossRef](#)]

Disclaimer/Publisher’s Note: The statements, opinions and data contained in all publications are solely those of the individual author(s) and contributor(s) and not of MDPI and/or the editor(s). MDPI and/or the editor(s) disclaim responsibility for any injury to people or property resulting from any ideas, methods, instructions or products referred to in the content.